Materials Chemistry and Physics 364 (2026) 132830

Contents lists available at ScienceDirect

Materials Chemistry and Physics

journal homepage: www.elsevier.com/locate/matchemphys

"Green" nanofibrous hydrogel loaded with pineapple-derived bromelain for enhanced wound healing

Anna Zakrzewska [a], Zuzanna J. Krysiak [a], Alicja Kosik-Kozioł [a], Daniel Rybak [a], Seyed Shahrooz Zargarian [a], Michele Zanoni [b], Chiara Gualandi [b,c,d], Filippo Pierini [a,*]

[a] Department of Biosystems and Soft Matter, Institute of Fundamental Technological Research, Polish Academy of Sciences, Pawińskiego 5B, 02-106, Warsaw, Poland
[b] Department of Chemistry "Giacomo Ciamician", University of Bologna, Via Gobetti 85, 40129, Bologna, Italy
[c] INSTM UdR of Bologna, University of Bologna, Via Gobetti 85, 40129, Bologna, Italy
[d] Interdepartmental Center for Industrial Research on Advanced Applications in Mechanical Engineering and Materials Technology, CIRI-MAM, University of Bologna, Viale Risorgimento 2, 40136, Bologna, Italy

HIGHLIGHTS

- Lemon juice low-temperature cross-linking adheres to "green chemistry" principles.
- Synergistic effect of bromelain and lemon juice provides antibacterial properties.
- Material exhibits pH-dependent swelling properties and unique photo-thermal response.
- Release of fruit components provides effective antioxidant activity during infection.
- Hydrogels are biocompatible and accelerate wound closure in the initial healing phase.

GRAPHICAL ABSTRACT

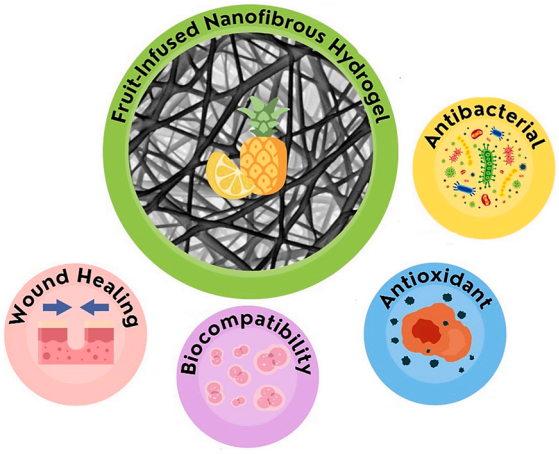

ARTICLE INFO

Keywords:
"Green" cross-linking
Lemon juice
Pineapple-derived bromelain
Electrospun nanofibers
Antibacterial hydrogel

ABSTRACT

The development of advanced poly(vinyl alcohol) (PVA)-based biomedical materials is often hindered by the reliance on toxic chemicals and energy-intensive processes, raising sustainability and safety concerns. This work addresses these challenges by presenting a low-temperature, "green" approach for fabricating PVA-based nanofibrous hydrogels cross-linked with natural lemon juice (*Citrus limon*) and enriched with bromelain derived from pineapple (*Ananas comosus*) extract. Electrospun nanofibers containing fruit components were stabilized via mild thermal treatment at 60 °C, enabling covalent ester bond formation while avoiding harmful cross-linkers and preserving the enzymatic activity of bromelain. Analysis results confirmed the successful formation of hydrogel, its reduced solubility in aqueous environments, improved mechanical properties, and

* Corresponding author.
E-mail addresses: azakrzew@ippt.pan.pl (A. Zakrzewska), zkrysiak@ippt.pan.pl (Z.J. Krysiak), akoziol@ippt.pan.pl (A. Kosik-Kozioł), drybak@ippt.pan.pl (D. Rybak), shzargar@ippt.pan.pl (S.S. Zargarian), michele.zanoni5@unibo.it (M. Zanoni), c.gualandi@unibo.it (C. Gualandi), fpierini@ippt.pan.pl (F. Pierini).

https://doi.org/10.1016/j.matchemphys.2026.132830
Received 3 March 2026; Received in revised form 24 May 2026; Accepted 19 June 2026

tunable pH-responsive swelling behavior. Bromelain incorporation altered cross-linking density, enhancing multifunctionality. The dual-bioactive hydrogel could release incorporated substances, demonstrating strong antioxidant capacity and antibacterial activity. Moreover, the developed nanofibrous hydrogel showed photothermal response under near-infrared (NIR) irradiation. *In vitro* assays using L929 fibroblasts demonstrated high biocompatibility and stimulated cell proliferation over extended culture periods. Moreover, the developed hydrogel supported early-stage wound closure, highlighting its importance in promoting the initial phases of the healing process, which are critical for effective tissue regeneration. By combining the natural bioactivities of lemon juice and bromelain with the structural advantages of electrospun PVA fibers, the developed nanoplatform offers a promising, environmentally friendly solution for advanced wound healing, bacterial elimination, and infection control applications.

1. Introduction

Poly(vinyl alcohol) (PVA) is a synthetic, water-soluble polymer [1] widely used in biomedical applications due to its biocompatibility [2], non-toxic nature, and good mechanical stability [3]. It contains numerous hydroxyl groups along its backbone, which not only make PVA highly hydrophilic [4], but also provide reactive sites for chemical modifications [5]. When subjected to cross-linking, either via chemical agents or through environmentally friendly, "green" approaches such as reactions with naturally derived acids, adjacent polymer chains become interconnected through covalent or physical bonds [6]. This transformation converts the linear or branched polymer [7] into a three-dimensional network known as a hydrogel [8]. Cross-linked PVA exhibits significantly improved mechanical strength, resistance to dissolution, and the ability to absorb and retain substantial amounts of water or biological fluids, thus mimicking human soft tissues [9]. Importantly, hydrogels possess semi-permeable characteristics, enabling the diffusion of small molecules, including therapeutic agents, while simultaneously blocking the penetration of larger molecules and harmful microorganisms [10,11]. This dual functionality aids tissue regeneration while minimizing the risk of infection. Additionally, their inherent softness and mechanical flexibility enable them to conform closely to surrounding tissues, which helps prevent mechanical irritation and enhances patient comfort, especially in wound healing dressing applications [12]. In this context, electrospun PVA nanofibrous hydrogels attract particular attention [13].

Electrospinning is a versatile fiber fabrication technique that utilizes a high-voltage electric field to draw a polymer precursor solution into ultrafine, continuous fibers, which are collected as a nonwoven mat on the grounded collector surface. The resulting fibrous structures have nanoscale diameters, a large surface-to-volume ratio, and high porosity, which makes them particularly beneficial for biomedical applications [13]. For instance, highly porous PVA networks can efficiently manage wound exudate while maintaining a moist environment favorable for healing [12]. Owing to its ease of processing, solubility in water, and favorable viscoelastic properties, PVA can be readily electrospun without the need for toxic solvents [14]. Moreover, its fiber morphology and final properties can be easily tailored by adjusting electrospinning parameters [14], blending with bioactive agents [15] and other polymers [16], or choosing a proper cross-linking method [17], making it an excellent platform for designing multifunctional, bioinspired materials.

To avoid the use of harmful chemicals not only during PVA processing but also during its cross-linking, recent research by Zakrzewska et al. has proposed "green" alternatives to the stabilization process, such as utilizing natural fruit-derived agents [7]. It was proven that lemon juice rich in citric acid (CA) and ascorbic acid (vitamin C) can catalyze low-temperature (60 °C for 7 days) esterification between hydroxyl groups of PVA chains and carboxyl groups of lemon juice, forming stable hydrogels with natural antioxidant properties and antibacterial effect against *Staphylococcus aureus* (*S. Aureus*). These properties are advantageous for wound dressings, particularly when inflammation and microbial contamination hinder tissue repair. What is additionally important, the development of low-temperature methods paved the way for the encapsulation of therapeutic substances, such as enzymes, within the "green" polymer matrix, without affecting their biological activity [7]. A slightly different approach was presented by Iqbal M. et al. [18] The authors prepared a sustainable halochromic sensor for real-time monitoring of chicken spoilage. The fabricated PVA-based electrospun nanocomposite contained an additive of eggshell membrane, lemon extract as a solvent and cross-linking agent, and was coated with ethanolic curcumin extract. The esterification reaction was carried out at 90 °C for 18 h [18]. A similar methodology was described in the work of Khalid M. et al. [19] The authors fabricated a face mask composed of PVA nanofibers and natural ingredients such as eggshell membrane and honey. The precursor solution was prepared using lemon juice as both the solvent and the cross-linking agent. The materials were heat-treated at 90 °C for one day [19].

In this study, we extend a previously developed sustainable, low-temperature cross-linked PVA/lemon juice nanofibrous platform by its enrichment with pineapple extract containing bromelain. Bromelain is a complex blend of proteolytic (protein-digesting) enzymes [20,21] known for its anti-inflammatory [20,22,23], antioxidant [21,24], antimicrobial [23,25], anticarcinogenic, and debriding activities [22,23], which can facilitate the removal of necrotic tissue and support regeneration. Incorporating bromelain into the PVA-based lemon juice-cross-linked nanofibrous matrix aimed to yield a multifunctional hydrogel that combines antioxidant action, antibacterial protection, and enzymatic bioactivity. The fabrication and characterization of a dual-bioactive electrospun material are described, and its potential as a next-generation wound dressing for enhanced wound healing is evaluated. The obtained hydrogel nanoplatform has reduced solubility in aqueous environments, confirming formation of covalent ester linkages that create and stabilize the polymer's three-dimensional structure. The nanoplatform is also characterized by improved mechanical properties manifested by a higher Young's modulus compared to the fibers not subjected to thermal treatment at 60 °C for 7 days (as-spun, ncl) and increased elasticity compared to the material without lemon juice addition (water-based one). Moreover, it was confirmed that both lemon juice and bromelain can be released from the nanofibrous matrix, showing strong antioxidant and antibacterial effects, especially against *S. Aureus*. Interestingly, the hydrogel exhibits a photothermal response when stimulated with near-infrared (NIR) light. The obtained results, together with the *in vitro* cell migration test, make the developed platform a robust candidate for wound healing applications, accelerating this process at an early stage.

2. Experimental section

2.1. Materials

Poly(vinyl alcohol) (PVA, M_w 85 000−124 000 Da, DH 99+%), ethanol absolute (EtOH), 50% (w/w) and 25% ((w/w), Grade I, specially purified for use as an electron microscopy fixative) glutaraldehyde solutions, phosphate buffer saline (PBS), 2,2-diphenyl-1-picrylhydrazyl (DPPH), L929 murine fibroblast cells (derived from adipose tissue), Triton X-100, bovine serum albumin (BSA), DAPI, hexamethyldisilazane (HMDS), and paraformaldehyde were purchased from Sigma-Aldrich (Poland). Fresh lemon (*Citrus limon*; imported from Spain) was

purchased from a local supermarket (Hale Banacha, Poland) and juiced (pH ≈ 2). Pineapple (*Ananas comosus*; derived from India) extract, standardized to a bromelain content of 2500 Gelatin Digesting Units (GDU) g^{-1}, was obtained from NANGA (Poland). Lysogeny broth (LB) and LB agar were bought from A&A Biotechnology (Poland). *Staphylococcus aureus* (*S. Aureus*, ATCC 6538, Gram-positive bacteria) and *Escherichia coli* (*E. Coli*, ATCC 25 922, Gram-negative bacteria) were purchased from Pol-AURA (Poland). Dulbecco's modified Eagle's medium (DMEM), fetal bovine serum (FBS), penicillin-streptomycin (PS), and ethylenediaminetetraacetic acid-trypsin (EDTA-trypsin) were bought from Gibco Invitrogen (USA). PrestoBlue and Alexa Fluor 488 Phalloidin were obtained from Thermo-Fisher Scientific (USA).

2.2. Methods

2.2.1. Fabrication of bromelain-enhanced PVA/lemon juice nanoplatform

Fresh lemon was squeezed to obtain fruit juice (L). To separate the remaining pulp, it was centrifuged for 5 min (15000 RPM) using a PHOENIX Instrument Micro Centrifuge CD-2012 and then filtered twice using syringe filters with polyethersulfone membranes: 0.45 μm and 0.20 μm, respectively. The electrospinning solution was prepared by dissolving PVA (10% (w/v)) in pure lemon juice (100% (v/v)) by heating at 80 °C for 2 h on a magnetic stirrer. After cooling the polymer solution, EtOH in a volume ratio of 1:9 (EtOH:lemon juice) and pineapple extract powder (P) containing bromelain (3% (w/v)) were added, and the vial was placed on a magnetic stirrer at room temperature (RT) for 15 min until complete dissolution. The concentration of bromelain was set at 3% (w/v) based on preliminary optimization studies, as higher concentrations were found to adversely affect the electrospinnability of the solution, leading to process instability and non-uniform fiber morphology. The precursor solution was electrospun, using an Inovenso NE300 NanoSpinner chamber, onto a drum collector surface wrapped with aluminum foil at RT and under ambient humidity. The collector distance from the 23G needle tip was 12 cm, the rotation speed was 400 RPM, the voltage was 13 kV, and the solution flow rate was 500 μl h^{-1}. In a similar manner, PVA/water (W) nanofibers containing pineapple extract, as well as PVA/lemon juice and PVA/water nanofibers without the enzyme, were also prepared, omitting the stage of its addition. The solutions were electrospun using the same process parameters. These samples were used for comparison purposes.

2.2.2. Cross-linking of nanoplatform

All of the prepared materials were divided into two parts: one was cross-linked (cl) and the other remained in its original, unchanged state (ncl). Due to the presence of the enzyme in some mats, the samples were subjected to mild "green" cross-linking conditions by placing them in an oven set at 60 °C for 7 days. This is the temperature at which bromelain does not lose its enzymatic activity [26,27], and the entire process ensures environmental safety. The development of this cross-linking method and its in-depth comparison with other approaches (including heating at 60 °C for 7 days for nanofibers without lemon juice addition) have been described previously in detail [7]. After 7 days, the nanofibers were removed from the oven and subjected to further analysis. Based on the solvent used and enzyme content in the fibers, the following codes were assigned to the samples.

cl-PVA-L—PVA/lemon juice nanofibers cross-linked at 60 °C for 7 days;
cl-PVA-LP—PVA/lemon juice/pineapple extract nanofibers cross-linked at 60 °C for 7 days;
cl-PVA-W—PVA/water nanofibers cross-linked at 60 °C for 7 days;
cl-PVA-WP—PVA/water/pineapple extract nanofibers cross-linked at 60 °C for 7 days.

The codes PVA-W, PVA-WP, PVA-L, and PVA-LP denote non-cross-linked (ncl) samples. At the stage of material optimization, samples subjected to cross-linking at 60 °C for 3 days were also prepared.

2.2.3. Determination of solubility

The fundamental analysis for determining the cross-linking efficiency of PVA-based materials is the solubility test in an aqueous environment. A 5.5 mg fragment was cut from each of cl-PVA-W, cl-PVA-WP, cl-PVA-L, and cl-PVA-LP mats and placed in a separate vial with 1 mL of PBS. The vials were closed and left at RT for 24 h. After this time, the nanofibrous hydrogels were removed for air-drying, followed by morphological characterization, and the supernatants were stored for spectrophotometric analysis. An analogous test was performed by incubating samples immersed in PBS at 37 °C, mimicking the human body temperature.

2.2.4. Morphological characterization

All nanofibrous hydrogels, both before and after solubility tests (removed from PBS after 24 h and freeze-dried overnight using Labconco 700401000 FreeZone), were analyzed using a scanning electron microscope (SEM, JSM-6010PLUS/LV, In TouchScope microscope) to evaluate their morphology. To provide the conductivity necessary for imaging, the samples were coated with a thin layer of gold using the DII-29030SCTR JEOL Smart Coater. All samples were examined at a beam energy of 5 kV, and images were captured at a 2500× magnification. Based on SEM images, the average porosity of the electrospun mats and pore size were calculated using ImageJ. Each image was analyzed three times.

2.2.5. Gel content

To evaluate the gel content of all four nanofibrous materials, approximately 10 mg samples were transferred into vials containing 10 mL of deionized (DI) water. They were allowed to soak for 2 h and subsequently mixed for 10 min on the magnetic stirrer. After mixing, the DI water was replaced with fresh solvent. This step was performed three times. The samples were then placed under vacuum for an hour to eliminate any residual moisture. Once dried, the samples were weighed, and the gel content, meaning the insoluble fraction of the PVA-based samples, was determined based on the mass retained.

2.2.6. Spectroscopic analysis

Attenuated Total Reflectance Fourier-Transform Infrared Spectroscopy (ATR-FT-IR) analysis was performed to identify functional groups and confirm the chemical composition of the nanofibrous samples, evaluate the degree of their cross-linking, and investigate the interaction of PVA hydrogel with pineapple-derived bromelain. The samples were scanned with a resolution of 2 cm^{-1} in the wavenumber range of 4000−400 cm^{-1} using a Vertex70, Bruker spectrometer, and OPUS 8.1 software.

Ultraviolet−Visible (UV−Vis) Spectroscopic analyses of lemon juice and bromelain (pineapple extract) solution were performed using a Multiscan GO absorption spectrometer (Thermo Scientific). To this end, several samples of lemon juice and bromelain at different concentrations were prepared. Prior to analysis, lemon juice solutions (0−8% (w/v) in PBS) were heated at 80 °C for 2 h following heating at 60 °C for 7 days, while bromelain solutions (0−6% (w/v) in PBS) were only heated at 60 °C for 7 days. These conditions reflected the processing of both substances at the stages of preparing precursor solutions for electrospinning and nanofiber cross-linking. UV−Vis spectra were recorded over the wavelength range of 200–1000 nm using a quartz cuvette.

Following the nanofiber solubility tests in PBS, the supernatants were analyzed spectrophotometrically using a Multiscan GO absorption spectrometer (Thermo Scientific) with a quartz cuvette. For each sample, the UV-Vis spectrum was recorded in the range of 200–1000 nm. These measurements aimed to assess whether, and to what extent, lemon juice components and bromelain were released into the aqueous medium after 24 h of immersion.

2.2.7. In vitro lemon juice and bromelain release studies

10 mg of each nanofibrous hydrogel (cl-PVA-L and cl-PVA-WP) was accurately weighed and transferred into separate test tubes (the cl-PVA-LP sample was excluded because two fruit-derived analytes exhibited overlapping absorbance peaks, preventing their individual quantification). An equivalent amount of pure PVA-based material (without additives; cl-PVA-W) was used as a control to remove any interference from the polymer matrices. 1 mL of fresh, preheated PBS (pH 7.4) was added to the testing tubes and incubated at 37 °C throughout the entire release process. At specified time intervals, the release medium was collected and replaced with fresh PBS. The absorbance of the withdrawn supernatant samples was measured using a UV–Vis spectrophotometer (Multiskan GO, Thermo Scientific, USA) at the maximum absorbance wavelengths specific to bromelain heated at 60 °C for 7 days (λ_{max} = 248 nm) and lemon juice heated at 80 °C for 2 h and at 60 °C for 7 days (λ_{max} = 279 nm). The concentration of released substances was quantified based on calibration curves prepared from the lemon juice (0−8% (w/v)) and bromelain (0−6% (w/v)) solutions in PBS.

2.2.8. pH-dependent swelling test

To investigate the absorption capacity of the developed hydrogels, pH-dependent swelling tests were conducted. It is possible that not all citric acid molecules participate in the esterification reaction, and the free carboxyl groups in the systems are responsible for their pH-responsivity [28]. Three samples of similar size were cut from each of the cl-PVA-L, cl-PVA-LP, cl-PVA-W, and cl-PVA-WP materials, weighed, and then placed in a separate vial into which 1 mL of PBS (pH = 7.1, 5.4, and 3.5) was pipetted. Subsequently, at several time points (1, 5, 15, 30, 60, 120, and 180 min), the samples were removed from the PBS solution and reweighed after lightly drying with a lint-free KimTech tissue. The last weighing measurement was taken 21 days after the initial measurement. To determine the swelling ratio at each time point, the following formula (Eq. (1)) was used:

$$Swelling\ ratio\ (\%) = \left(\frac{w_{wet\_t} - w_{dry}}{w_{dry}}\right) \times 100 \qquad \text{(Eq. 1)}$$

w_{wet_t}—mass of the wet sample removed from water after time t, and w_{dry}—mass of the dry sample before immersion in water (t_0).

After that, the samples were freeze-dried overnight (Labconco 700401000 FreeZone), sputtered with a thin layer of gold (DII-29030SCTR JEOL Smart Coater), and imaged using SEM (JSM-6010PLUS/LV, In TouchScope microscope; beam energy of 5 kV, 1000× magnification).

2.2.9. Thermal properties

Thermogravimetric analysis (TGA) was conducted to examine the changes in the mass of the material sample as a function of temperature. The measurements were performed using a TA Instruments TGA Q500, heating from RT to 600 °C at a rate of 10 °C min^{-1} under a nitrogen atmosphere.

Differential scanning calorimetry (DSC) measurements were carried out on a TA Instruments Q100 system equipped with an RCS90 refrigerated cooling unit. The analysis involved an initial heating cycle from −90 °C to 240 °C at a rate of 20 °C min^{-1}, subsequent cooling down to −90 °C at 10 °C min^{-1}, and a final reheating phase up to 240 °C at 20 °C min^{-1}.

2.2.10. Crystalline structure

To determine the crystalline structure of cl-PVA-LP nanofibrous hydrogel, an X-ray diffraction (XRD) analysis was performed. For this purpose, a PANalytical X'Pert PRO diffractometer equipped with a fast solid-state X'Celerator detector was used. The analysis was carried out at RT using Cu Kα radiation (40 mA, 40 kV). Data were collected over a 2θ range of 5–50°, with a step size of 0.033° and a counting time of 20 s per step. The cl-PVA-L sample was then analyzed in the same way.

2.2.11. Mechanical properties

Mechanical testing was performed on all bromelain-containing samples, including both non-cross-linked materials (as-spun, ncl) and those cross-linked at 60 °C for 3 and 7 days. Tensile strength was evaluated using a CTX Texture Analyzer (Brookfield Ametek). From each material, three strips measuring 1 cm × 4 cm were cut, mounted in the grips of the analyzer, and stretched until the breaking point. The initial gauge length of each sample was set to 2 cm. Data acquisition was performed at a rate of 50 points s^{-1}, with a trigger load of 0.10 N and a constant elongation speed of 1 mm s^{-1}. Force–displacement curves were recorded using Texture Pro V1.0 Build19 software, and these were subsequently used to calculate and plot stress–strain relationships. Stress was defined as the applied force divided by the initial cross-sectional area of the sample, while strain was expressed as the change in length relative to its initial value [29]. Young's modulus, representing the material's stiffness, was determined as the slope of the stress–strain curve within the linear elastic region, reflecting the ratio of stress to strain under elastic deformation [30]. For each material, Young's modulus was calculated by averaging the results from three repetitions.

2.2.12. Photothermal response

To assess the influence of bromelain on the photoresponse of the system, NIR laser irradiation (MDL-H-808/5W, Changchun New Industries Optoelectronics Tech. Co., Ltd.) at a wavelength of 808 nm and power densities of 2.5, 3.5, and 4.5 W/cm^2 was applied. The tests were performed on nanofiber mats (cl-PVA-W, cl-PVA-WP, cl-PVA-L, and cl-PVA-LP), from which equally sized samples were cut, as well as on pineapple extract powder. Each material was irradiated until it reached and stabilized at its maximum temperature. After 150 s, the laser was switched off to allow the materials to cool. Temperature changes throughout the experiment were monitored using a thermal imaging camera (FLIR A655sc, EC TEST Systems) in conjunction with FLIR Research Studio software.

2.2.13. Antioxidant properties

To determine the antioxidant capacity of pineapple-derived bromelain and the developed cl-PVA-LP nanofibrous hydrogel, the DPPH method was employed. Initially, only lemon juice and pineapple extracts were analyzed in order to establish their intrinsic antioxidant properties and obtain a reference for further comparisons. This step was necessary to eliminate any possible influence of the electrospun matrix on the measured activity of the nanostructured platforms.

Lemon Juice and Pineapple Extract. In the first stage of the test, lemon juice and pineapple extract (bromelain) samples were prepared in a 24-well plate. For this purpose, a 0.1 mM ethanolic DPPH solution and PBS were added to pure lemon juice, both immediately after preparation (not-heated, NH) and after heating at 80 °C for 2 h (H), to obtain juice solutions with concentrations of 1% and 10% (v/v). Bromelain solutions (enzyme heated at 60 °C for 7 days) were prepared at concentrations of 1%, 3%, 5%, and 10% (w/v). The DPPH solution concentration was 50% (v/v) in each case, with the remainder being PBS. The samples were analyzed spectrophotometrically using a Multiscan GO absorption spectrometer (Thermo Scientific) after incubation for 1, 2, and 24 h at 37 °C.

cl-PVA-L and cl-PVA-LP nanofibrous hydrogels. In the second stage of the test, fragments weighing 5.5 mg and 11.0 mg were excised from each of the analyzed materials (cl-PVA-L and cl-PVA-LP). The samples were then placed in vials with 1 mL of PBS for 24 h at RT or 37 °C. After this time, 1%, 10%, and 20% (v/v) supernatant solutions were prepared in a 24-well plate by adding 0.1 mM ethanolic DPPH solution and PBS. The DPPH solution concentration was 50% (v/v) in each case. Therefore, the DPPH/PBS/supernatant ratio was 50/49/1 (1% (v/v) supernatant), 50/40/10 (10% (v/v) supernatant), and 50/30/20 (20% (v/v) supernatant). Samples were incubated at 37 °C for 1, 2, and 24 h and subjected to spectrophotometric analysis using a Multiscan GO absorption spectrometer (Thermo Scientific).

The absorbance maximum of an ethanolic DPPH solution diluted in PBS (50/50) was determined as 507 nm. Therefore, when determining the antioxidant capacity of the tested samples, measurements were performed for this specific wavelength. The absorbance value was used to calculate the lemon juice, bromelain, cl-PVA-L, and cl-PVA-LP supernatants' free radical inhibition capacity, depending on their concentration. The following formula (Eq. (2)) was used [31].

$$Inhibition\ (\%) = \left(\frac{A_0 - A_t}{A_0}\right) \times 100 \quad \text{(Eq. 2)}$$

A_0—absorbance of the DPPH solution without the presence of an antioxidant (oxidized state), and A_t—absorbance of the DPPH solution with the presence of an antioxidant (reduced state) after incubation at 37 °C.

2.2.14. Antibacterial effect

Prior to microbial studies, samples were placed in the 96-well plates and sterilized under UV light for 30 min on each side. The antibacterial properties of cl-PVA-L and cl-PVA-LP were verified both quantitatively and qualitatively. *E. Coli* (ATCC 25 922) and *S. Aureus* (ATCC 6538) were isolated from culture with a streak plate method and inoculated in 3 mL of LB. Both suspensions were incubated overnight in an orbital shaker at 37 °C. The next day, bacterial suspensions were diluted in sterile PBS to obtain 10^6 colony-forming units (CFU) mL^{-1}.

Quantitative Antibacterial Activity. For the quantitative study, 100 μL of the given bacteria suspension was added to the cl-PVA-L and cl-PVA-LP samples placed in the 96-well plate and incubated for 3 h at 37 °C. The bacterial suspension alone was used as a positive control (CTRL). After that time, 100 μL of sterile PBS was added to each well, and the bacterial suspension was gently mixed. Then, 100 μL of the solution was transferred to the 96–well plate, serially diluted from 10 to 100 000 in 10-fold steps, and plated on LB agar plates, which were incubated overnight at 37 °C. All the samples were tested in triplicate and with three technical repetitions. Bacterial survival was analyzed by counting bacterial colonies.

Qualitative Antibacterial Activity. For the qualitative study, a zone inhibition test was performed. The 100 μL of *S. Aureus* and *E. Coli* suspensions (10^6 CFU mL^{-1}) were spread onto agar plates. The cl-PVA-L and cl-PVA-LP samples measuring 9 mm in diameter were placed on the agar plates and incubated at 37 °C overnight. Representative photos were captured the following day. For the control (CTRL), agar plates without electrospun fibers were used.

2.2.15. Cell studies

Culturing L929 Fibroblast Cells. L929 murine fibroblast cells were cultured in DMEM supplemented with 10% (v/v) FBS and 1% (v/v) PS, and maintained in an incubator at 37 °C with 5% CO_2. The culture medium was changed every two days. Cells were passaged when they reached approximately 80% confluence. For seeding, cells were detached by incubation with 0.05% EDTA-trypsin at 37 °C with 5% CO_2 for 3 min. The cells were collected in a Falcon tube, centrifuged at 1200 RPM for 5 min to form a pellet, resuspended in 1 mL of culture medium, and counted.

Sterilization and Seeding of Samples. Fibrous samples from four groups, cl-PVA-W, cl-PVA-WP, cl-PVA-L, and cl-PVA-LP, were electrospun onto coverslips with a diameter of 1.5 cm and sterilized using 30-min UV light exposure on each side. Samples were rinsed three times with PBS. The samples were then placed in 24-well plates, where L929 fibroblast cells were seeded onto the fibrous samples at a density of 10^4 cells per sample. As a control (CTRL), tissue culture plates were also seeded at the same cell density. The samples were cultured for up to 7 days.

Cell Viability. Cell viability was assessed using the PrestoBlue assay. All groups of fibrous samples (cl-PVA-W, cl-PVA-WP, cl-PVA-L, and cl-PVA-LP) and the control (CTRL) were treated with a solution containing 10% (v/v) PrestoBlue reagent in the culture medium and incubated for 1 h at 37 °C with 5% CO_2. Following the incubation, 100 μL aliquots of the PrestoBlue solution were transferred to a 96-well plate and analyzed using a Fluoroskan Ascent™ Microplate Fluorometer (Thermo Scientific) with an excitation wavelength of 530 nm and an emission wavelength of 620 nm. Five samples were tested per group, with two readings taken from each sample at three specific time points: 1, 3, and 7 days after seeding.

Cell Morphology. The morphology of L929 fibroblasts seeded on the samples was assessed using SEM (JSM-6010PLUS/LV, In TouchScope microscope) at 7 days and confocal microscopy (Leica) at 3 and 7 days post-cell seeding. To conduct SEM imaging, the preparation started by fixing the cells seeded onto fibrous samples (cl-PVA-L and cl-PVA-LP) and onto coverslips (CTRL) in 3% (v/v) ice-cold glutaraldehyde (Grade I) for 20 min. Subsequently, the cells were washed three times with deionized water and dehydrated by immersing them in ethanol solutions of increasing concentrations (50%, 70%, 90%, and 100% (v/v)) for 15 min each. HMDS was then applied to the cells, which were left to air-dry overnight under a fume hood. Finally, the samples were sputter-coated with a thin layer of gold using a DII-29030SCTR JEOL Smart Coater.

To conduct confocal visualization, the samples were initially washed with PBS and then fixed in 4% (v/v) paraformaldehyde for 2 h at RT. The cell cytoskeleton (actin) and nuclei were stained by fixing the samples in 4% (v/v) paraformaldehyde for 15 min at RT. The samples were then washed three times with PBS and treated with a 0.1% (v/v) Triton X-100 solution for 15 min. After another wash, the samples were incubated in a solution of 1% (w/v) BSA with 0.1% (v/v) Triton X-100 for 1 h. Subsequently, the samples were washed and incubated with a mixture containing 1% (w/v) BSA, 0.1% (v/v) Triton X-100, and a 1:40 solution of Alexa Fluor 488 Phalloidin for 1 h in the dark. Finally, the nuclei were stained by adding a 1:500 DAPI solution in PBS for 10 min. After washing three times, the cell cytoskeleton and nuclei were visualized using a confocal microscope.

Cell Migration Tests. L929 murine fibroblast cells were seeded at a concentration of 7000 cells mL^{-1} in specialized cell migration culture plates, which featured a silicon insert to separate two compartments (Culture-insert 2 Well 24, ibiTreat, Ibidi, Martinsried, Germany). According to the manufacturer's instructions, 70 μL of the cell suspension was added to each side of the well, divided by the silicon insert, and incubated at 37 °C with 5% CO_2 until they covered the compartments. Then, the silicon insert was removed, and the cells were treated with sample extracts (cl-PVA-L and cl-PVA-LP) and normal medium (CTRL). The extract was obtained following the ISO 10993-12:2021 standard [32]: cl-PVA-L and cl-PVA-LP hydrogels were weighed to achieve a standard extraction ratio of 0.2 g mL^{-1}. The samples were sterilized, washed five times with PBS, and then placed in DMEM supplemented with FBS and PS for 24 h at 37 °C with 5% CO_2. After this incubation period, the extracts were collected and further sterilized using a 0.2 μm filter. The distance between the cells in the two compartments was observed using a confocal microscope (Leica) until the gap was completely closed by the cells. The tests were performed for triplicate inserts for each group.

2.2.16. Statistical analysis

Data are presented as mean ± standard deviation. Statistical analysis was performed using one-way ANOVA test, and differences were considered significant at $p \leq 0.05$ (*$p \leq 0.05$, **$p \leq 0.01$, ***$p \leq 0.001$, ****$p \leq 0.0001$).

3. Results and discussion

The fabrication process of electrospun hydrogel enriched with bromelain from pineapple extract (cl-PVA-LP), cross-linking mechanism, and system performance are shown in Scheme 1. For comparison purposes, nanofibrous hydrogels containing the enzyme but not lemon

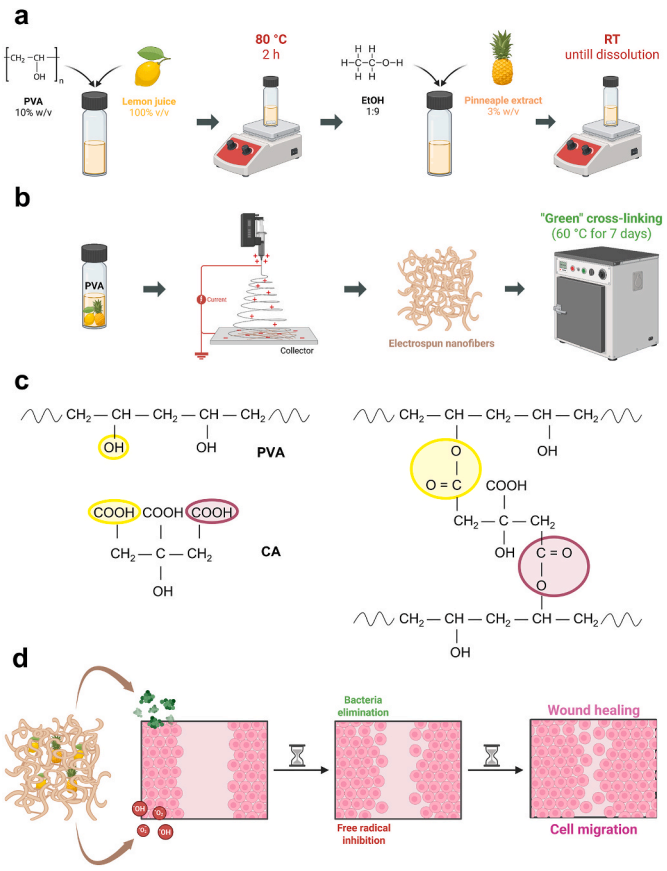

Scheme 1. Schematic diagram of the fabrication of electrospun cl-PVA-LP nanofibrous hydrogel and system performance. a) Two-step preparation of the precursor solution for electrospinning: dissolution of PVA in lemon juice by stirring at 80 °C for 2 h, followed by the addition of EtOH and pineapple-derived bromelain dissolved at RT. b) Electrospinning of the precursor solution and mild cross-linking of the obtained nanofibers at 60 °C for 7 days. c) Possible mechanism of cross-linking PVA nanofibers using natural lemon juice. An esterification reaction occurs between the hydroxyl groups (−OH) of the polymer (PVA) and the carboxyl groups (−COOH) of citric acid (CA). d) Fabricated system combats bacteria, scavenges free radicals, and supports cell migration, improving the wound healing process at its early stage.

juice (cl-PVA-WP), as well as hydrogels without the enzyme (cl-PVA-L and cl-PVA-W), were also fabricated. As a result of temperature-induced cross-linking, the samples containing lemon juice turned slightly yellow (Fig. S1), suggesting chemical changes in composition, which has been previously reported [7]. The cross-linking method used was already described in detail and developed for the incorporation of biologically active molecules, such as enzymes, into a PVA polymer matrix [7]. The prepared materials represent nanofibrous hydrogels with high potential for biomedical applications, especially wound healing, due to their antioxidant, anti-inflammatory, and antibacterial properties; therefore, they were extensively characterized in this regard.

3.1. Nanoplatforms' solubility and morphological characterization

The solubility test was the initial method used to verify whether the nanofibers had been successfully cross-linked, forming hydrogels. Since highly cross-linked PVA forms an insoluble network, visual assessment of the material after immersion in water or PBS provides a preliminary indication of the cross-linking efficiency. In this study, none of the analyzed samples (cl-PVA-L and cl-PVA-LP) dissolved, suggesting a successful stabilization process and allowing the materials removed from PBS after 24 h to be subjected to SEM analysis. Microscopic images of both the as-prepared samples and those after 24-h solubility tests at RT and 37 °C are shown in Fig. 1a and b. The analysis confirmed that the as-prepared materials consist of continuous nanofibers with a cylindrical shape and random orientation. In both cases, no beads were observed. Moreover, samples have similar porosity and pore size (cl-PVA-L: 41.1 ± 0.3% and 0.347 ± 0.002 μm; cl-PVA-LP: 41.8 ± 5.1% and 0.382 ± 0.058 μm). SEM images of materials after solubility tests provided valuable insights, demonstrating that the applied cross-linking procedure effectively stabilizes the PVA-based nanofibrous structures. Indeed, after 24 h immersion in PBS, both at RT and 37 °C, the fibrous morphology of both cl-PVA-L and cl-PVA-LP samples remained clearly visible, confirming the successful cross-linking of the polymer matrix and its resistance to dissolution. The fibers in both hydrogels appeared more compact and interconnected after incubation, which may be attributed to swelling and rearrangement within the cross-linked network. The porosity and pore size of cl-PVA-L and cl-PVA-LP after immersion in PBS at RT were 15.4 ± 0.2%, 0.093 ± 0.001 μm and 32.1 ± 2.8%, 0.033 ± 0.002 μm, respectively. An interesting inversion of the porosity and pore size trends was observed when the incubation temperature increased to the physiological level. For the cl-PVA-L, the total porosity increased from 15.4 ± 0.2% (at RT) to 31.3 ± 2.5% (at 37 °C), while the average pore size simultaneously decreased from 0.093 ± 0.001 μm to 0.044 ± 0.015 μm. This behavior can be potentially attributed to the thermally accelerated release of unreacted, water-soluble components derived from lemon juice. At 37 °C, the extensive release of fruit ingredients from the polymer matrix likely generated a higher density of newly formed, interconnected micro-voids, thereby increasing the overall porosity despite the reduction in pore dimensions. In contrast, the bromelain-containing nanofibrous hydrogel (cl-PVA-LP) exhibited a significant reduction in both porosity (14.6 ± 3.2%) and pore size (0.015 ± 0.003 μm) at 37 °C compared to RT. Given that 37 °C represents the physiological optimum for stem bromelain, the elevated temperature enhances polymer chain mobility and may induce conformational alterations in the protein structure. The incorporation of pineapple extract containing bromelain (cl-PVA-LP) did not hinder the cross-linking process; the fibrous structure was retained, and the material remained insoluble after 24 h exposure to PBS. This suggests that the extract components can participate in or even enhance cross-linking interactions, contributing to the morphological stability of the samples. The above statement is also evidenced by the fact that PVA nanofibers containing only pineapple extract (cl-PVA-WP) achieved better dissolution resistance than the cl-PVA-W control sample, confirming that this fruit component favors the polymer cross-linking (Fig. S2a and b). This is further supported by the results of the bromelain-enriched polymeric films' stability in aqueous medium. As shown in Fig. S3, the PVA-WP and PVA-LP films (not subjected to any cross-linking treatment) do not dissolve completely after 24 h of immersion. In the case of the second sample, the release of lemon juice and enzyme can be suspected as partially responsible for its greater mass loss. While bromelain facilitates the cross-linking process, its role is much more multifaceted. As a complex mixture of proteolytic enzymes, it may act as a macromolecular filler that promotes hydrogen bonding between the PVA chains or alters the kinetics of the esterification through local pH micro-environments. Due to the heterogeneous nature of the pineapple extract, a singular chemical reaction cannot be definitively assigned.

3.2. Gel content

Quantitative analysis of the insoluble hydrogel fraction revealed that the cl-PVA-LP exhibited the highest degree of cross-linking, which supports the conclusions drawn from the PBS solubility tests. Moreover, the results confirm that bromelain enhances cross-linking not only in the lemon juice-containing samples (cl-PVA-L vs. cl-PVA-LP) but also in the water-based ones (cl-PVA-W vs. cl-PVA-WP). The gel content was determined as: 45.13 ± 2.17% for cl-PVA-W; 51.73 ± 1.62% for cl-PVA-WP; 73.43 ± 1.07% for cl-PVA-L; 79.86 ± 2.57% for cl-PVA-LP.

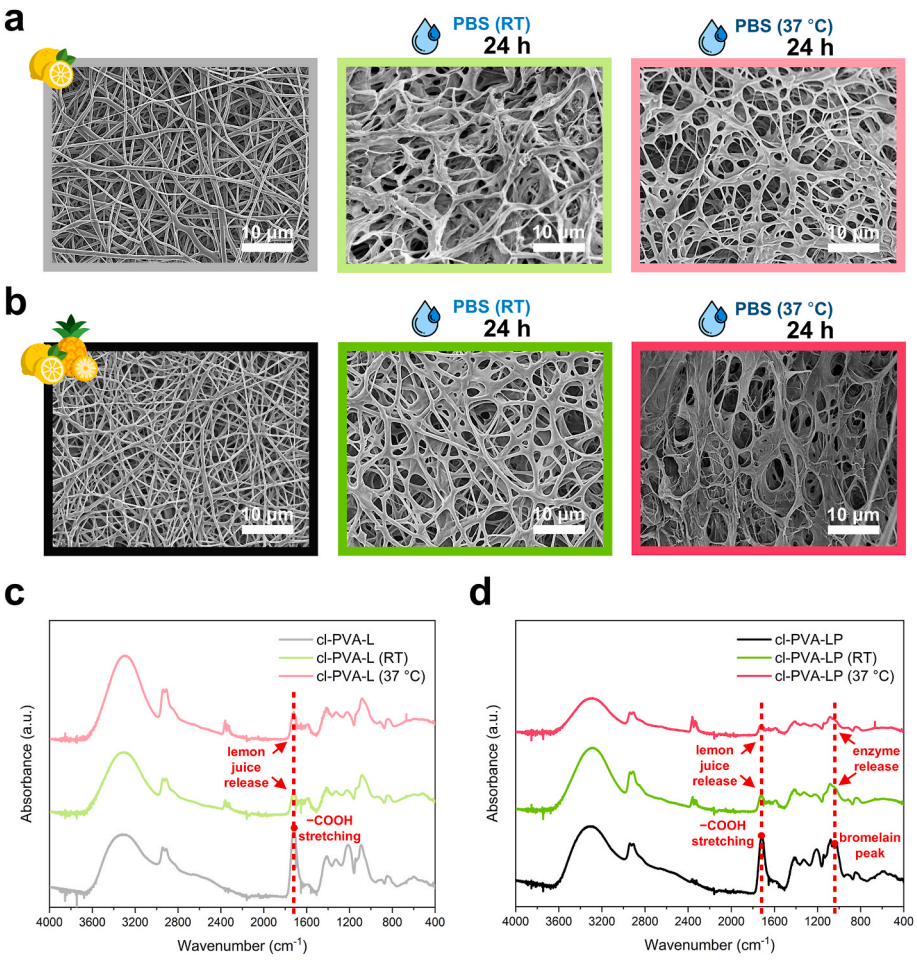

Fig. 1. Morphological and spectroscopic analysis of nanofibrous hydrogels before and after solubility tests. a) SEM micrographs of hydrogel containing lemon juice (cl-PVA-L) before solubility test (left), after 24 h in PBS at RT (center), and at 37 °C (right). b) SEM micrographs of hydrogel containing lemon juice and bromelain (cl-PVA-LP) before solubility test (left), after 24 h in PBS at RT (center), and at 37 °C (right). The images confirm successful cross-linking. c) ATR-FT-IR spectra of cl-PVA-L hydrogel before and after immersion in PBS at RT and 37 °C, confirming release of lemon juice. d) ATR-FT-IR spectra of cl-PVA-LP hydrogel before and after immersion in PBS at RT and 37 °C, confirming release of lemon juice and bromelain. The active substances exit the nanofibers regardless of the medium temperature.

3.3. Spectroscopic analysis

Attenuated Total Reflectance Fourier-Transform Infrared Spectroscopy (ATR-FT-IR). ATR-FT-IR analysis enabled the identification of functional groups in the developed nanoplatforms and the determination of the effect of bromelain or other components of pineapple extract on the PVA nanofibrous hydrogel enriched with lemon juice. In the cl-PVA-L and cl-PVA-LP spectra (Fig. 1c and d), the broad peak with a maximum at 3315 cm^{-1} and 3305 cm^{-1}, respectively, is attributed to the extensive hydrogen bonding network and corresponds to the stretching vibrations of hydroxyl (−OH) groups [15]. The two peaks at 2943 and 2907 cm^{-1} are associated with the symmetric and asymmetric stretching vibrations of methylene ($-CH_2$) groups [33]. The peak observed at 1717 cm^{-1} is characteristic of carboxyl group stretching (comprising carbonyl –C═O and hydroxyl –OH units) and results from the presence of citric acid in the lemon juice [7,34]. The band at 1412 cm^{-1} is related to deformation vibrations of $–CH_2$ groups [35], while the one at 1326 cm^{-1} arises from bending vibrations of $–CH_2$ and –OH [36]. A small peak at 1257 cm^{-1} can be assigned to the stretching of –C–O– bonds within secondary alcohol groups [37], whereas the peaks at 1143 and 1090 cm^{-1} correspond to −C–O–C− stretching vibrations, characteristic of acetal (ether) linkages, formed, *i.a.*, during cross-linking [38]. The band around 1024 cm^{-1} appears only in the cl-PVA-LP hydrogel and can be attributed to bromelain, as confirmed by the spectrum of pineapple extract powder standardized for a specific content of this enzyme (Fig. S4a). The C–O stretching in the –OH group and/or the −C–O–C− (ether group) stretching, typical of sugars, causes the mentioned peak [39]. Bromelain is a glycoprotein, *i.e.*, a protein containing covalently bound sugar residues [40]. After the solubility tests, the majority of peaks exhibit a slight decrease in intensity, indicating potential rearrangement of the PVA network structure or partial dissolution of the insoluble fraction [7]. What is particularly important, ATR-FT-IR analyses suggest that both lemon juice and bromelain are released from the nanoplatforms after immersion in PBS for 24 h, as evidenced by the significant reduction of the peak at 1717 cm^{-1} (Fig. 1c and d) and the absence of the peak at 1024 cm^{-1} (Fig. 1d), respectively. Analogous spectra for samples without lemon juice (cl-PVA W and cl-PVA-WP) are shown in Fig. S2c and d. These results further confirm the release of the enzyme into the aqueous medium regardless of the incubation temperature. The observed reduction in the intensity of the peak at 1717 cm^{-1} after incubation is attributed to the gradual release of lemon juice components into the medium. This decrease is consistent with the intended functional profile of the scaffold, which aims to provide sustained antioxidant activity at the wound site through the controlled release of bioactive substances.

A critical comparison between the non-cross-linked and thermally treated samples reveals evidence of covalent bond formation (esterification). Specifically, a displacement of the two principal functional groups is observed upon cross-linking (Fig. S4b). First, the sharp peak at 1715 cm^{-1} (PVA-L), assigned to the stretching vibrations of the free

carboxyl groups from citric acid in the lemon juice, shifts to 1717 cm^{-1} in both cl-PVA-L and cl-PVA-LP. This shift is characteristic of the formation of aliphatic ester carbonyl (C═O) bonds. Second, the broad stretching band of the hydroxyl groups around 3307 cm^{-1} for PVA-W undergoes a notable reduction in relative intensity and a distinct displacement, confirming the chemical consumption of the –OH groups from PVA during the esterification reaction.

Ultraviolet–Visible (UV–Vis) Spectroscopy. Full UV–Vis spectra of lemon juice and pineapple bromelain were recorded to define the absorption peak maximum, necessary for further analyses, including the determination of release profiles from nanofibrous matrices. For both substances, the solutions were heated prior to spectrophotometric analysis to best mimic the processing conditions during the preparation of the precursor solutions, and thus the form in which they would be found in PBS medium after release from the hydrogels. As shown in Fig. 2a, lemon juice, after heating at 80 °C for 2 h and then at 60 °C for 7 days, exhibits an absorption maximum at 279 nm, whereas pineapple extract, heated at 60 °C for 7 days, absorbs radiation at a wavelength of 248 nm. Importantly, heating shifts the absorption peak of bromelain toward shorter wavelengths, with the peak centered at 277 nm for the not-heated pineapple extract solution (Fig. S5a). Such a blue shift is typically associated with the temperature dependence of aromatic residue peak positions and often indicates an enhanced exposure of aromatic side chains to the solvent during thermal treatment [41]. This suggests a partial conformational rearrangement of the protein within the PVA matrix. Nevertheless, the cross-linking conditions do not have a negative effect on the enzymatic activity of bromelain, which is preserved, as confirmed by the gelatin digestion test result (Fig. S5b). It should be noted that the absorption bands at 279 nm (corresponding to the presence of lemon juice) and 248 nm (corresponding to the presence of bromelain) represent the collective absorbance of each of these complex fruit-derived additives, comprising hundreds of phytochemicals and proteolytic enzymes, rather than individual chemical species. Based on the absorbance values for differently concentrated solutions of either heated lemon juice or bromelain from pineapple extract, calibration curves were plotted (Fig. S6). In the next step, supernatants after 24-h solubility tests of cl-PVA-L, cl-PVA-LP, cl-PVA-W, and cl-PVA-WP in PBS at different temperatures (RT and 37 °C) were subjected to spectrophotometric analysis. UV–Vis spectra for samples with and without lemon juice are presented in Fig. 2b. In the case of cl-PVA-L and cl-PVA-LP, an intense peak at 279 nm is observed in the spectra, confirming the release of lemon juice into the medium, with a greater amount released at 37 °C compared to RT. Furthermore, the mentioned peak is less intense in the samples incorporating bromelain, and the characteristic peak for this enzyme is absent, which may be due to the interference of signals from both analyzed substances. This conclusion is supported by spectral analysis of samples cl-PVA-W and cl-PVA-WP, where a peak at 248 nm is observed, indicating the enzyme leaching from the nanofibrous hydrogel. In this case, a low-intensity peak at approximately 279 nm may indicate partial decomposition of the polymer matrix. To determine the precise release profiles of lemon juice and bromelain from the hydrogels, an additional test was performed.

3.4. *In vitro* lemon juice and bromelain release studies

In vitro release studies quantified the release of lemon juice and bromelain from the nanofibrous hydrogels. The release profile of lemon juice was determined using the cl-PVA-L sample, while bromelain release was assessed with the cl-PVA-WP sample. This test was not carried out on the cl-PVA-LP sample because, as demonstrated above, overlapping absorbance signals from the two fruit-derived components prevent reliable quantitative determination of their individual release. Both substances follow a diffusion-controlled release mechanism, but at different rates (Fig. 2c). The release of lemon juice is gradual, with the most rapid increase occurring within the first 8 h. After just 1 h, its concentration in the release medium reaches 3.1% (v/v) (31 μL released), and after 8 h, it is 17.4% (v/v) (174 μL released). Beyond this point, the release slows, reaching 20.6% (v/v) (206 μL released) after 72

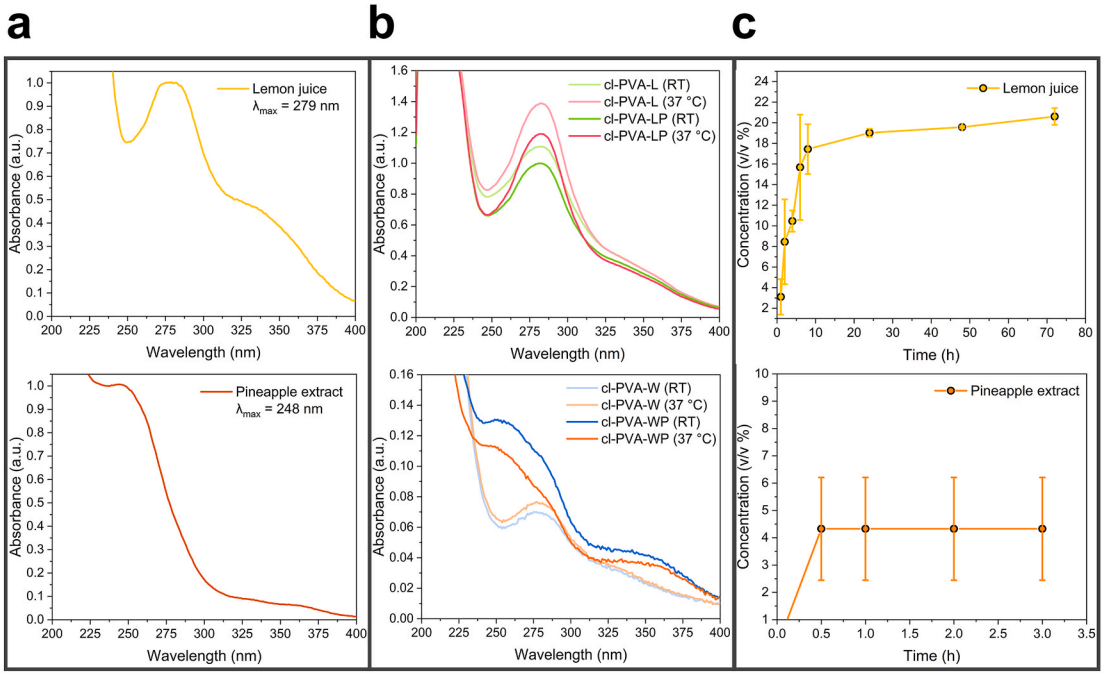

Fig. 2. Spectroscopic analysis of supernatants after solubility tests and release profiles of active substances from hydrogels. a) Representative UV–Vis spectra of lemon juice heated at 80 °C for 2 h and then at 60 °C for 7 days (top) and pineapple extract rich in bromelain after heating at 60 °C for 7 days (bottom). The absorption maximum is at wavelengths of 279 nm and 248 nm, respectively. b) UV–Vis spectra of supernatants after cl-PVA-L and cl-PVA-LP solubility tests (top), as well as cl-PVA-W and cl-PVA-WP solubility tests (bottom). The presence of characteristic peaks in the spectra confirms the release of lemon juice and bromelain from the nanofibrous hydrogels, both at RT and 37 °C. c) Release profiles of lemon juice (top) and bromelain (bottom) into PBS medium. Lemon juice releases gradually over time, while the enzyme release is burst.

h. In contrast, bromelain exhibits a completely different release behavior. In the case of the cl-PVA-WP sample, a burst release is observed, achieving a maximum bromelain concentration of 4.3% (w/v) (43 mg released) in the release medium within only 30 min. This can probably be attributed to the lower cross-linking density in hydrogels without lemon juice, as well as those containing the enzyme. Consequently, it can be assumed that bromelain release from the cl-PVA-LP hydrogel would be slower, although this cannot be directly quantified with the available methods.

3.5. pH-dependent swelling test

Due to the possibility that the cl-PVA-L and cl-PVA-LP hydrogels may contain unreacted carboxyl groups derived from lemon juice (not all of which participate in the esterification reaction during cross-linking), they were tested for swelling capacity at different pHs. Indeed, the tested hydrogels exhibited a clear dependence of the swelling ratio on the environmental pH, confirming the presence of ionizable –COOH groups in the polymer matrix (Fig. 3a and b). In an acidic environment (pH 3.5), the carboxyl groups of citric acid are largely in the undissociated –COOH form, since the pH is close to the first dissociation constant ($pKa_1 \approx 3.44$) [42]. This protonated state limits electrostatic repulsion between polymer chains, keeping the hydrogel structure compact and resulting in lower swelling. As the pH of the environment increases above the second and third pKa values of citric acid ($pKa_2 \approx 5.02$, $pKa_3 \approx 6.55$) [42], more –COOH groups deprotonate into negatively charged $-COO^-$ species. The increased negative charge enhances electrostatic repulsion among polymer chains, causing the loosening of the network and increased water binding. Consequently, swelling is the highest in the neutral (pH 7.1) or slightly alkaline environments. For cl-PVA-L, swelling at pH 3.5, 5.4, and 7.1 reached near-maximum values within a few minutes of immersion in PBS and remained stable for 21 consecutive days, ultimately reaching 1082 ± 43%, 1230 ± 74%, and 1479 ± 34%, respectively (Fig. 3c). In case of samples containing bromelain (cl-PVA-LP), lower swelling degrees were observed across the entire pH range tested compared to samples with lemon but without the enzyme. This can be attributed to a higher degree of cross-linking in nanofibers containing pineapple components, which restricts the mobility of the polymer chains. Additionally, stem bromelain, as a protein with a positive charge at pH values below its isoelectric point (pI ≈ 9.5) [27], partially neutralizes the negative charges of the $-COO^-$ groups in the hydrogel, reducing interchain repulsion and limiting network stretching. As a result, hydrogels with bromelain swell less intensely than their counterparts without the enzyme. However, similarly to cl-PVA-L, the samples reached almost the maximum swelling after just a few minutes of PBS immersion. After 21 days at pH levels of

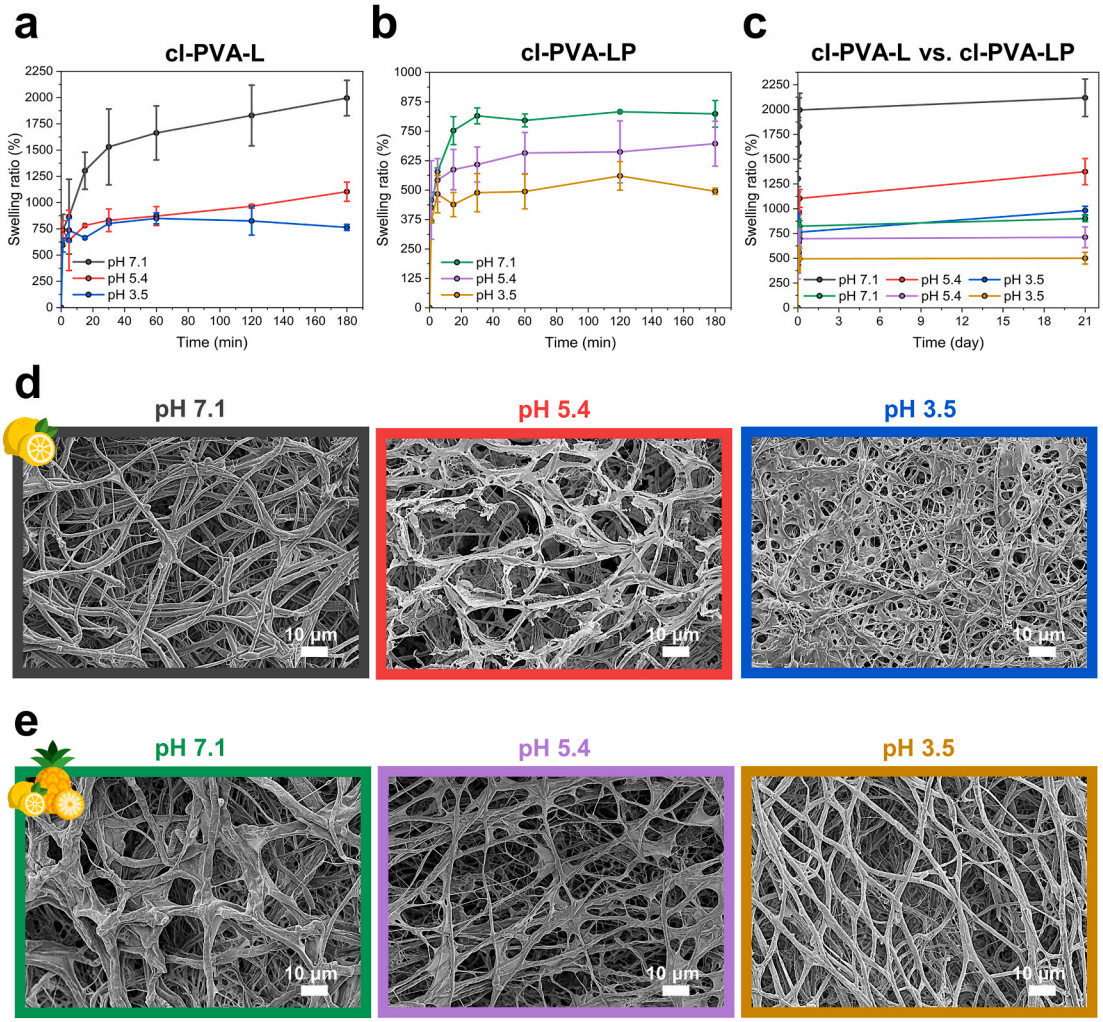

Fig. 3. Analysis of pH-responsivity of nanofibrous hydrogels. a) Swelling of cl-PVA-L and b) cl-PVA-LP hydrogels at different pH levels for up to 3 h. c) Comparison of swelling rates of cl-PVA-L and cl-PVA-LP hydrogels over 21 days. The results confirm the pH-responsivity of the hydrogels, which absorb more PBS as the pH increases. The presence of bromelain significantly affects the swelling of the PVA-based hydrogel, reducing it due to the positive protein charge in the tested pH range. SEM micrographs of d) cl-PVA-L and e) cl-PVA-LP nanofibrous hydrogels after 21 days in a medium varying in pH (pH = 7.1, 5.4, and 3.5).

3.5, 5.4, and 7.1, the percentages were 601 ± 60%, 862 ± 48%, and 982 ± 57%, respectively (Fig. 3c). Importantly, the swelling test results at pH 7.1 (RT) correlate well with the porosity values of the materials after 24-h immersion in PBS (RT). For the cl-PVA-L sample, which showed the highest swelling degree under these conditions, a rapid decrease in porosity was observed from approximately 41.1% to 15.4%. This is a direct result of the significant increase in the volume of individual nanofibers that filled the voids. In the case of cl-PVA-LP, the limited swelling of the hydrogel allowed for significantly better preservation of the porous structure, showing a porosity of approximately 32.1% after immersion (41.8% before solubility test).

To verify the effect of the swelling degree of the nanofibrous hydrogels on their morphology, the samples were analyzed using SEM after 21 days of testing. Despite the leaching of soluble, bioactive components indicated by spectroscopic analyses, the nanofibrous morphology remained intact throughout the 3-week period. This duration is considered optimal for wound healing applications, particularly for supporting the critical early stages of tissue regeneration. Microscopic images of the cl-PVA-L (Fig. 3d) revealed that the fibrous morphology of these nanohydrogels was best preserved at pH 7.1, suggesting that the covalent cross-links and hydrogen-bonding interactions within the PVA/lemon juice network were strong enough to maintain structural integrity despite a high degree of swelling under these conditions. At lower pH values, the reduced ionization of carboxyl groups and partial protonation of hydroxyl groups likely weakened the intermolecular interactions, resulting in fiber coalescence and surface deformation. A different effect was observed for the cl-PVA-LP (Fig. 3e). The incorporation of bromelain significantly altered the pH-dependent behavior of the material: the fibers were best preserved at pH 3.5, whereas at pH 5.4 and 7.1, the fibrous structure was deformed. It can be assumed that at pH 5.4 and 7.1, when the –COOH groups partially or fully dissociate into $-COO^-$, the local ionic repulsion in the matrix is greater, the fibers swell more, and become more susceptible to deformation. Bromelain, being a positively charged protein in this pH range, can bind to anionic $-COO^-$ groups, disrupting the uniform charge distribution and weakening the stabilizing hydrogen bonds within the fibers. At pH 3.5, the carboxyl groups mainly remain in the undissociated state (−COOH), which reduces electrostatic repulsion and stabilizes the structure. Bromelain positive interactions are less significant in these conditions, and the fibers remain stable. The above-mentioned lower swelling degree of cl-PVA-LP samples compared to cl-PVA-L samples further supports this hypothesis, indicating the neutralization of some anionic charges by positively charged bromelain and its stiffening effect by reducing ionic repulsion within the network.

3.6. Thermal properties

TGA measurements were conducted to evaluate the thermal stability of the nanofibrous hydrogels and to examine the thermal decomposition behavior of their individual components. Fig. 4a illustrates the temperature-dependent mass changes of the cl-PVA-L and cl-PVA-LP samples, while Fig. 4b shows the corresponding first derivative curves. Both nanoplatforms exhibit a slight weight loss around 30–80 °C, attributed to the evaporation of moisture adsorbed on the nanofiber surfaces. A further mass reduction is observed between 100 and 220 °C, corresponding to the degradation or volatilization of lemon juice ingredients. The most significant mass loss, associated with the depolymerization and breakdown of the polymer backbone, occurs within the 220–380 °C range. In addition, the cl-PVA-LP sample exhibits a minor weight loss around 250–275 °C, likely associated with the thermal decomposition of protein molecules through pyrolysis of amino acid residues. At temperatures above 400 °C, the remaining organic

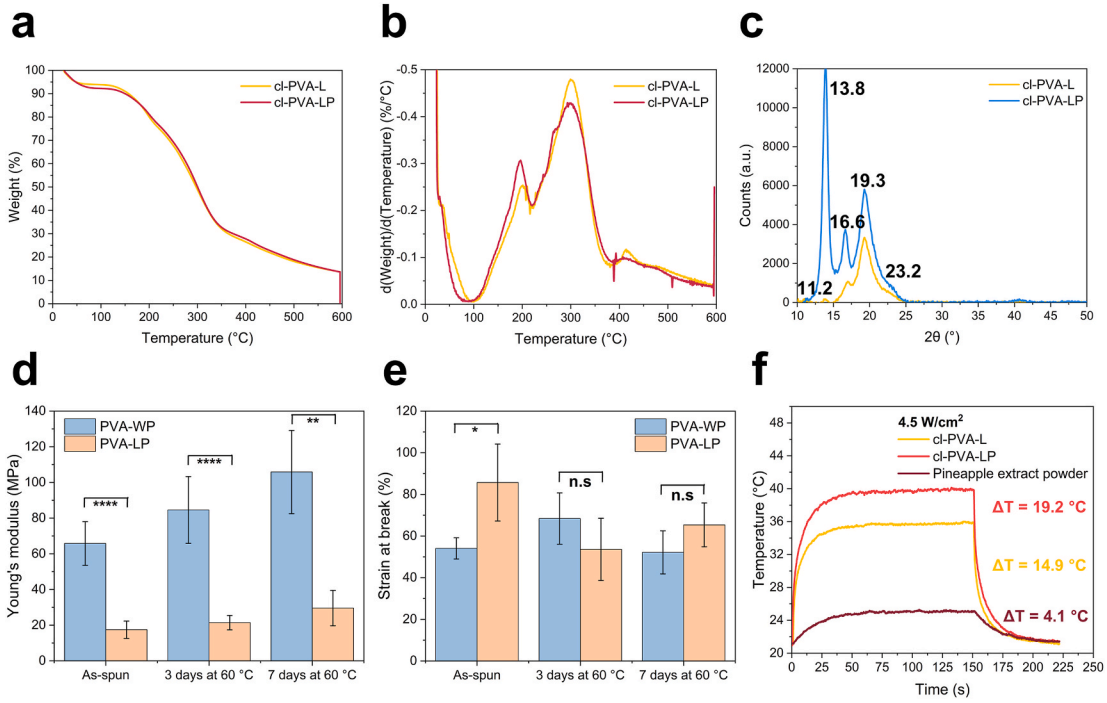

Fig. 4. Thermal, structural, mechanical, and photoresponsive properties of the developed nanofibrous hydrogels. a) TGA curves showing mass change over time for material containing lemon juice (cl-PVA-L) and lemon juice with pineapple extract (cl-PVA-LP). b) First derivative of the TGA curve. Substantial weight loss is observed for cl-PVA-L and cl-PVA-LP hydrogels at temperatures above 100 °C. c) XRD patterns of cl-PVA-L and cl-PVA-LP. Both nanofibrous hydrogels are semi-crystalline. d) Young's modulus and e) strain at break of nanofibrous samples: as-spun (ncl) and treated at 60 °C for 3 or 7 days (the latter corresponds to the cl-PVA-WP and cl-PVA-LP samples). Longer cross-linking time improves mechanical properties by increasing stiffness. Improvements in mechanical properties are also evident in increased strain at break compared to samples without lemon juice. f) Photothermal response of cl-PVA-L and cl-PVA-LP under the influence of NIR irradiation at a power density of 4.5 W/cm^2 (RT). Although pineapple extract in powder form does not exhibit photothermal properties, the cl-PVA-LP sample can absorb radiation and convert it into heat.

fragments undergo decomposition, after which the TGA curves reach a plateau, indicating the completion of major degradation processes.

As demonstrated above, the cl-PVA-L and cl-PVA-LP hydrogels exhibit substantial weight loss at temperatures above 100 °C. This limited thermal stability hinders the ability to obtain reliable data from differential scanning calorimetry (DSC), as shown in Fig. S7.

3.7. Crystalline structure

XRD analysis demonstrates the presence of a crystalline phase in the nanofibrous hydrogels cl-PVA-L and cl-PVA-LP, as shown in Fig. 4c. In both samples, the main diffraction peak appears at $2\theta \approx 19°$, accompanied by additional peaks at $2\theta \approx 11°$ and 23°, which are characteristic of the crystalline regions of PVA, confirming the semi-crystalline nature of both hydrogels. Peaks observed near $2\theta \approx 14°$ and 17° can be attributed to citric acid, which is abundant in lemon juice [7]. Bromelain, in contrast, does not exhibit the characteristic diffraction peaks of crystalline materials.

3.8. Mechanical properties

Tensile tests were performed to determine the mechanical properties of bromelain-loaded nanofibrous hydrogels. The tests compared samples with varying degrees of cross-linking, *i.e.*, those with and without lemon juice, as well as those subjected to cross-linking for 3 or 7 days. Fig. 4d shows the Young's modulus values of the analyzed materials, providing information about their stiffness. Importantly, samples without lemon juice (PVA-WP) exhibited higher stiffness compared to those enriched with lemon juice (PVA-LP), which was observed for both non-cross-linked (as-spun, ncl) and cross-linked materials. This difference may be caused by the presence of citric acid in PVA-LP samples, which, in addition to promoting cross-linking, acts as a plasticizer by interpenetrating between PVA chains, disrupting hydrogen bonding, and reducing chain order [43]. As a result, polymer chains' mobility increases, lowering material stiffness [44]. This phenomenon is further evidenced by the representative stress-strain curves for cl-PVA-WP and cl-PVA-LP, which illustrate a distinct shift in material toughness (Fig. S8). As expected, the stiffness of both PVA-WP and PVA-LP samples increased with cross-linking density (longer heating time). It is essential to note that, as previously reported [7], this trend differs for samples without added enzyme. Before cross-linking, the lemon juice-enriched material (PVA-L) is softer compared to the material without the fruit component (PVA-W; effect of plasticization by citric acid). Then, cross-linking increases its (cl-PVA-L) stiffness compared to the cl-PVA-W sample, due to the formation of a denser network rich in ester bonds [7]. Therefore, it can be assumed that in the presence of pineapple extract, lemon juice acts in synergy with bromelain, being not only a plasticizer but also modifying the microstructure of the network, and reducing its macroscopic stiffness. This occurs despite a higher degree of cross-linking in cl-PVA-LP compared to cl-PVA-L, cl-PVA-W, and cl-PVA-WP. In contrast, in the water-based system, bromelain promotes the formation of a more uniform and compact network, resulting in greater stiffness, which is consistent with the higher cross-linking density of cl-PVA-WP compared to cl-PVA-W.

In summary, the results indicate that the presence of citric acid in the PVA matrix has a dual effect. Prior to cross-linking, it reduces the material's stiffness due to its plasticizing effect, while after cross-linking, it increases the material's stiffness due to its role as a cross-linking agent. The presence of bromelain modifies these effects by interacting with the components of lemon juice, influencing the material's microstructure and/or the distribution of the bonds formed.

Another parameter analyzed based on tensile tests is strain at break, which represents the maximum percentage elongation of a given material before its breaking point (Fig. 4e). The results show that the as-spun (ncl) sample containing both lemon juice and bromelain exhibits a significantly higher elongation at break (85.7 ± 18.5%) than the sample with bromelain only (54.1 ± 5.1%). This again indicates that the presence of lemon juice increased the initial plasticity of the material [44]. After 3 days at 60 °C, the PVA-WP strain at break increased slightly (to 68.4 ± 12.3%), while the PVA-LP elongation decreased (53.6 ± 14.9%). This can be interpreted as indicating that, in the PVA-WP sample, cross-linking was relatively incomplete, and the material remained quite flexible. However, in the PVA-LP sample, some of the citric acid had begun to react with the PVA (forming ester bonds), stiffening the structure and reducing its strain. In contrast, after 7 days at 60 °C, the elongation decreases in both samples, being higher for cl-PVA-LP (65.4 ± 10.5%) than for cl-PVA-WP (52.1 ± 10.3%). This suggests that over time, the cross-linking process in the cl-PVA-LP sample stabilizes at a level that still allows some flexibility due to the incomplete conversion of all citric acid groups, whereas the cross-linking in cl-PVA-WP continues, albeit at a slower rate. Prolonged heating of the materials clearly has a positive effect on the degree of cross-linking. It is worth noting that the number of bonds formed at this stage strengthens the material's structure, but not to the extent of significantly restricting the mobility of the polymer chains.

3.9. Photothermal response

As previously demonstrated [7], the cl-PVA-L nanofibrous hydrogel exhibits a certain photothermal response upon irradiation with near-infrared light (NIR, 808 nm, 2.5 W/cm^2). This photoresponsivity can be attributed to the formation of unsaturated double bonds, resulting from prolonged heating [45], used to initiate the cross-linking reaction. As a result, the fibers undergo a color change, enhancing their absorption of NIR light, which is subsequently converted into heat [7]. Pineapple extract powder and samples containing lemon juice and enriched with pineapple-derived bromelain were also tested for photothermal properties. An 808 nm NIR laser and a thermal imaging camera were used for this purpose. NIR radiation is frequently used in various biomedical applications due to its low absorption (by hemoglobin, melanin, and water) [46] as well as low scattering in the skin [47]. Under appropriate conditions, including radiation power density, this allows it to penetrate deeper tissues without posing a threat.

The photothermal response of cl-PVA-L, cl-PVA-LP, and pineapple extract alone to NIR irradiation of three different power densities is presented in Fig. 4f and Fig. S9a and b. In each case, the initial temperature was around 21.0 °C. As a result of irradiation of bromelain in powder form, no particular photothermal response is observed, even for a laser power density of 4.5 W/cm^2 ($\Delta T = 4.1$ °C). This is as expected, because the enzyme does not contain NIR-active chromophores or form absorbing structures. A different behavior is observed for the cl-PVA-L and cl-PVA-LP samples, which absorb an increasingly greater amount of energy with increasing laser power density. This results from the fact that the higher the power density, the more photons fall on the surface per second, so more energy enters the material in the same time. In the case of the cl-PVA-L hydrogel, the temperature change (ΔT) after NIR irradiation of 2.5, 3.5, and 4.5 W/cm^2 is 4.7, 9.9, and 14.9 °C, respectively. Interestingly, the cl-PVA-LP, despite the lack of enzyme photoresponsivity, absorbs a larger amount of radiation compared to the cl-PVA-L material, reaching up to 40.1 °C after NIR irradiation of 4.5 W/cm^2. For cl-PVA-LP, the temperature change (ΔT) relative to the initial temperature after NIR irradiation of 2.5, 3.5, and 4.5 W/cm^2 is 5.3, 12.1, and 19.2 °C, respectively. Therefore, it appears that a new phase of aggregates or complexes forms in the PVA matrix and the lemon juice environment, which disperses or absorbs NIR and converts it into heat. This phenomenon is extremely promising and requires further investigation, for example, in terms of antibacterial applications. The photothermal response of cl-PVA-W and cl-PVA-WP after irradiation with NIR laser at the same power densities (Figure S9c,d and Figure S10) further confirms that both lemon juice and pineapple extract play a substantial role in the scaffold's light-to-heat conversion efficiency.

3.10. Antioxidant properties

It has already been proven that cl-PVA-L hydrogel possesses antioxidant properties due to the presence of lemon juice rich in vitamin C and flavonoids [7]. These molecules act as reducing agents, neutralizing reactive oxygen species (ROS) and free radicals that can otherwise cause oxidative damage to cellular components, including lipids, proteins, and DNA [48]. By donating electrons to these reactive species, the antioxidants in lemon juice help to stabilize them and prevent the propagation of oxidative chain reactions. Similarly, bromelain, a proteolytic enzyme complex derived from pineapple (*Ananas comosus*), exhibits notable antioxidant properties in addition to its well-known anti-inflammatory and proteolytic activities. Bromelain has been shown to reduce lipid peroxidation [49,50] and to enhance the activity of endogenous antioxidant enzymes, such as superoxide dismutase [50,51] and catalase [51], thereby maintaining cellular redox balance. By mitigating oxidative damage to biomolecules, bromelain contributes to the protection of cells and tissues, supporting its potential therapeutic role in conditions associated with excessive oxidative stress. The DPPH method, used in this study to determine the antioxidant properties of lemon juice, bromelain, and nanofibrous hydrogels cl-PVA-L and cl-PVA-LP, utilizes the ability of antioxidants to reduce the stable nitrogen radical DPPH [52]. In its oxidized state, DPPH has a characteristic purple color and absorbs radiation at around 517 nm. After electron transfer from the antioxidant (free radical reduction), the DPPH color changes to yellow, resulting in a decrease in absorbance intensity at the same wavelength [7]. The general reaction mechanism between the DPPH radical and phenolic compounds (ArOH), the active antioxidants present in both lemon juice and pineapple extract, is presented in Fig. 5a.

Fig. 5b shows the color changes of DPPH solutions in the presence of lemon juice and bromelain after 1, 2, and 24 h of incubation. Lemon juice, both heated at 80 °C for 2 h (H) and non-heated (NH), is a strong antioxidant, as evidenced by the immediate color change of DPPH solutions from purple to yellow right after mixing. This effect is particularly visible after the use of 10% (v/v) juice. After 1 h of incubation, a high degree of reduction of DPPH by 1% (v/v) NH lemon juice occurs, and after 2 h, this process is already visible by 1% (v/v) H lemon juice. The %inhibition by lemon juice was calculated based on spectrophotometric analysis and presented in Fig. 5c and d. After 2 h of incubation, the % inhibition for 1% (v/v) H and NH juice is 84.7 ± 1.4% and 93.0 ± 0.6%, respectively. In the case of 10% (v/v) H and NH juice, it is 90.3 ± 0.4% and 90.7 ± 2.3%, respectively. Longer incubation does not have a

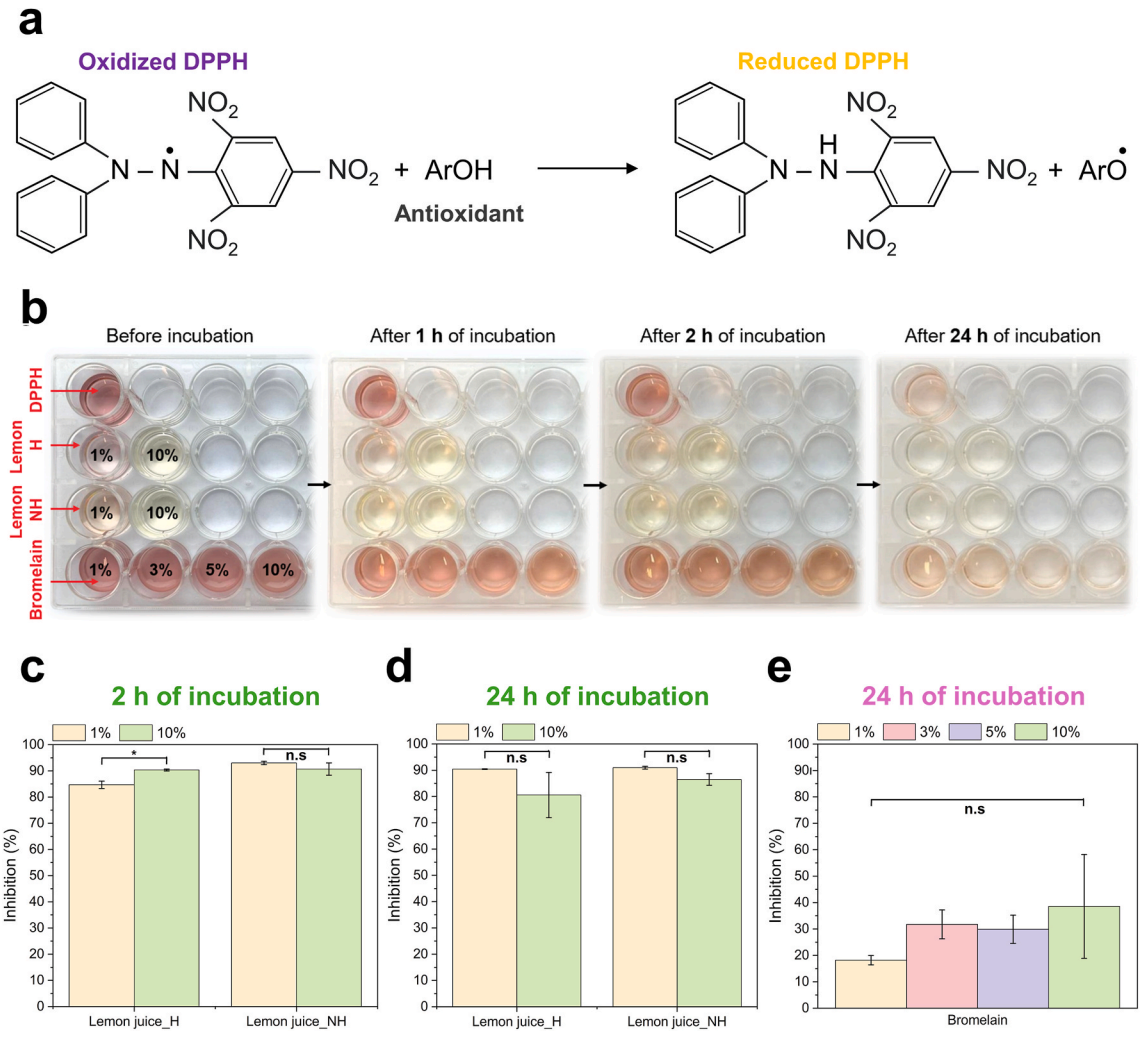

Fig. 5. Determination of the antioxidant properties of lemon juice and bromelain. a) General mechanism of DPPH radical reduction with phenolic compounds (ArOH), which are the active antioxidants present in both lemon juice and pineapple extract. As a result of the reaction, a color of DPPH change from purple to yellow. b) Visual assessment of the ability of lemon juice heated at 80 °C for 2 h (H) and without heat treatment (NH) to reduce the free radical DPPH. c) Inhibition of free radical DPPH by lemon juice at 1% and 10% (v/v) concentration after 2 h, and d) 24 h of incubation at 37 °C. e) Inhibition of free radical DPPH by bromelain at 1%, 3%, 5%, and 10% (w/v) concentration after 24 h of incubation at 37 °C. Both analyzed substances have the ability to inhibit free radicals, with lemon juice being a stronger antioxidant. (For interpretation of the references to color in this figure legend, the reader is referred to the Web version of this article.)

significant effect on the results, and it can be stated that the standard time of 2 h is sufficient. A different situation is observed for bromelain. Immediately after mixing the enzyme solutions with DPPH, no changes are observed (Fig. 5b). A clear antioxidant effect is visible only after 24 h of incubation, when the solution changes color to yellow due to DPPH reduction. As shown in Fig. 5e, the %inhibition under the influence of 1%, 3%, 5%, and 10% (w/v) bromelain is 18.2 ± 1.8%, 31.7 ± 5.5%, 29.9 ± 5.3%, and 38.6 ± 19.6%, respectively. In summary, bromelain is definitely a weaker antioxidant than lemon juice, primarily due to its lower content of classical compounds with strong reducing potential, such as vitamin C and polyphenols. Nevertheless, its antioxidant activity has been demonstrated and remains significant, as it helps protect cells against oxidative stress and may complement the action of other substances with antioxidant properties.

In the next step, the supernatants after immersion of cl-PVA-L and cl-PVA-LP hydrogel (HG) samples in PBS for 24 h (at RT and 37 °C) were examined. Visual observation indicates that a 10% (v/v) solution of each supernatant in DPPH (after releasing lemon juice and bromelain from 5.5 mg of hydrogel into 1 mL of PBS) causes a significant reduction of the free radical after only 1 h of incubation (Fig. 6a). This effect is increasingly stronger with time, also for 1% (v/v) supernatant. As shown in Fig. 6b and c, for both materials, the %inhibition increases with increasing supernatant concentration, but the temperature of active substances release from nanofibrous hydrogels does not significantly affect the antioxidant properties of the supernatant. There is also no visible difference between the materials with and without the addition of the enzyme, so again, it can be stated that the enzyme begins to act as an antioxidant after a longer time and requires 24-h incubation. The % inhibition values for cl-PVA-L and cl-PVA-LP are presented in Table S1. The graphs showing %inhibition of samples without lemon juice and bromelain (cl-PVA-W, cl-PVA-WP) are shown in Fig. S11.

3.11. Antibacterial effect

Lemon juice possesses natural antibacterial properties due to the content of citric acid and other antimicrobial compounds, such as flavonoids [53]. The juice's low pH (≈ 2) acidifies the environment, inhibiting the growth of many bacteria, especially acid-sensitive pathogens such as *E. Coli* or *Salmonella*. Furthermore, the antioxidants in its composition can damage bacterial cell membranes and disrupt their metabolism [54]. These features make lemon juice a commonly used natural preservative and hygiene aid. To confirm the antibacterial effect of lemon juice and to investigate the impact of bromelain on these properties, tests with cl-PVA-L and cl-PVA-LP were carried out using Gram-positive (*S. Aureus*) and Gram-negative (*E. Coli*) bacteria.

The quantitative studies demonstrated that both cl-PVA-L and cl-PVA-LP exhibit antibacterial activity against *S. Aureus* and *E. Coli*, although with varying degrees of intensity depending on the strain (Fig. 7a and b). In the case of the hydrogel without bromelain addition (cl-PVA-L), a decrease in *S. Aureus* survival to 48.4 ± 6.0% and *E. Coli* to 40.6 ± 37.9% is observed. This result suggests that the acidic pH and compounds present in lemon juice, such as citric acid and ascorbic acid, destabilize bacterial metabolism and disrupt the integrity of cell membranes, thereby inhibiting their growth. The significantly higher sensitivity of *E. Coli* compared to *S. Aureus* in the presence of lemon juice may be due to the greater susceptibility of the outer membrane of Gram-

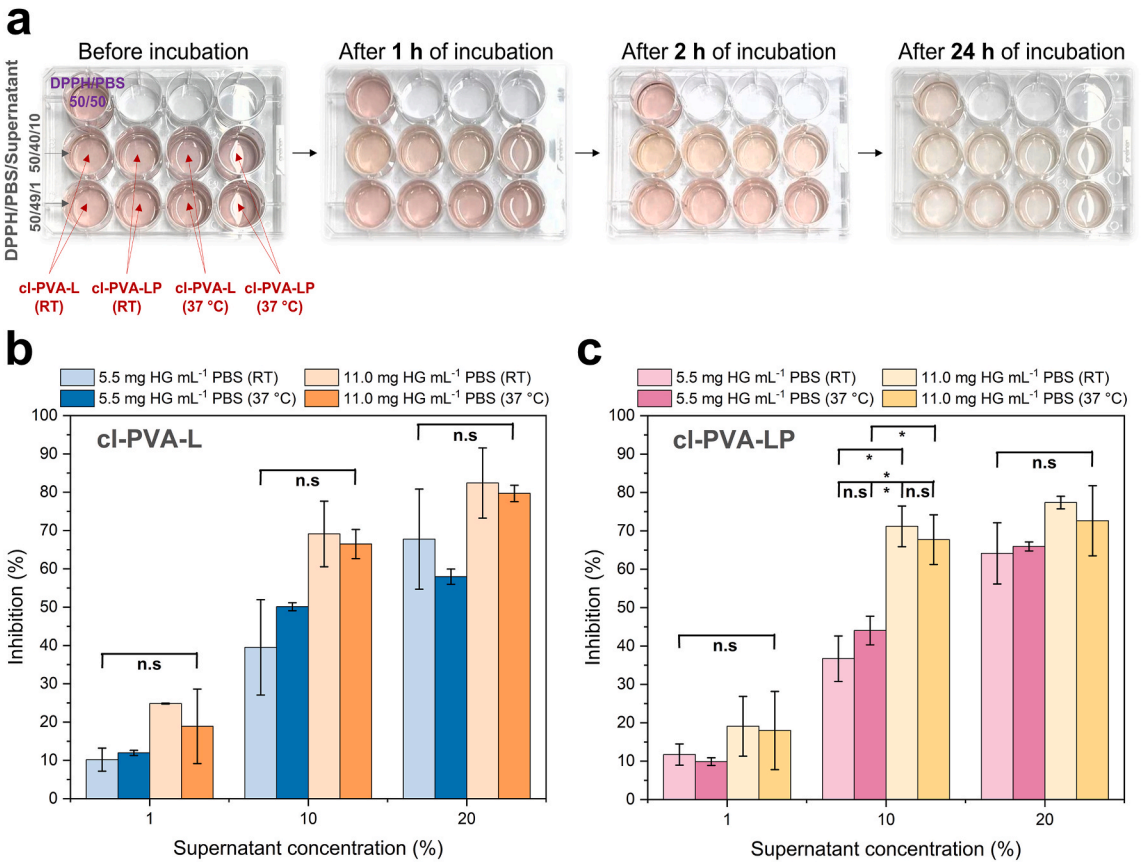

Fig. 6. Determination of the antioxidant properties of supernatants after hydrogels' (HG) solubility test. a) Visual assessment of the ability of cl-PVA-L and cl-PVA-LP supernatants to reduce the free radical DPPH. b) Inhibition of free radical DPPH by cl-PVA-L and c) cl-PVA-LP supernatants (after immersion in PBS at RT and 37 °C for 24 h) at 1%, 10%, and 20% (v/v) concentration after 2 h of incubation at 37 °C. Lemon juice and bromelain released from the nanofibers impart outstanding antioxidant properties to the supernatants. As expected, the %inhibition increases with increasing supernatant concentration and initial weight of the hydrogel sample. A more significant effect of bromelain could be seen after a longer incubation time.

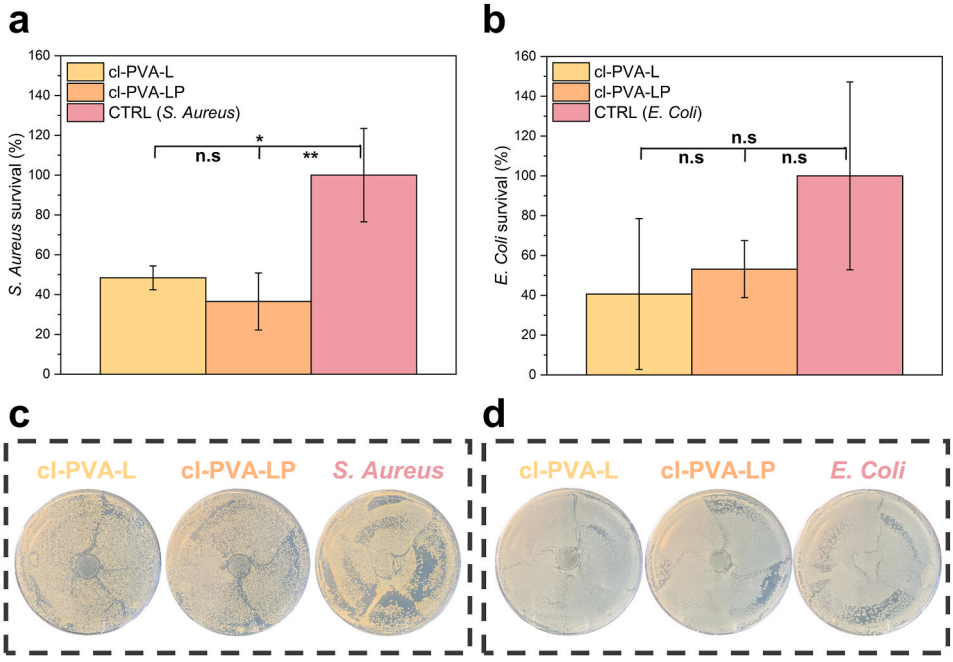

Fig. 7. Antibacterial properties of the developed hydrogel. a) Quantitative survival of *S. Aureus* and b) *E. Coli* after 3 h of incubation (37 °C) with cl-PVA-L and cl-PVA-LP. Bromelain synergizes with lemon juice against Gram-positive bacteria, possibly by degrading *S. Aureus* surface proteins and biofilm, enhancing citric acid penetration and activity. c) Zones of growth inhibition for *S. Aureus* and d) *E. Coli* on LB agar plates containing cl-PVA-L and cl-PVA-LP. Lemon juice and bromelain cannot penetrate the agar plate effectively; however, in the case of *S. Aureus*, a noticeably larger zone of inhibition is observed.

negative bacteria to environmental acidification and destabilization by hydrogen ions. The addition of bromelain to the system altered the antibacterial activity of the nanofibrous hydrogel. In the presence of cl-PVA-LP, *S. Aureus* survival decreased significantly to 36.5 ± 14.4%, while *E. Coli* survival increased to approximately 53.1 ± 14.3%. These results suggest that bromelain acts synergistically with lemon juice against Gram-positive bacteria, likely due to its proteolytic activity, which degrades the surface proteins and biofilm of *S. Aureus*, facilitating hydrogen ion penetration and the action of citric acid. However, in the case of *E. Coli*, the addition of bromelain appears to reduce the effectiveness of lemon juice, perhaps due to unfavorable interactions between the enzyme and outer membrane components or by partially neutralizing the acidic environment through proteolytic products. These differences may result from variations in cell wall structures and resistance mechanisms between the two bacterial groups tested.

The antibacterial effect of the samples was also assessed qualitatively after an overnight incubation of cl-PVA-L and cl-PVA-LP on agar plates inoculated with bacteria (Fig. 7c and d). The antibacterial effect of both samples was noticeable, with slightly higher zone inhibition observed for *S. Aureus*. The weaker antibacterial activity observed in qualitative tests compared with quantitative analyses may result from the limited diffusion of active compounds. During incubation on solidified agar at 37 °C, the cl-PVA-L and cl-PVA-LP hydrogels do not efficiently release lemon juice or bromelain from the structure, preventing their effective penetration into the agar and consequently reducing the inhibition of bacterial growth [32].

3.12. Cell studies

To evaluate the biological properties of the proposed fibrous matrices and their potential for biomedical applications, the interaction of these materials with L929 fibroblast cells was studied. The research focused on the effects of cl-PVA-L and cl-PVA-LP nanofibrous hydrogels on cell proliferation and morphology. Proliferation testing was also performed for water-based samples (cl-PVA-W and cl-PVA-WP). From day 1, significant differences were observed between the fibrous sample groups and the control (CTRL), indicating that fewer cells were initially attached to the surface of the fibrous samples. Interestingly, even the samples electrospun from water-based solutions (cl-PVA-W and cl-PVA-WP) showed slightly lower initial cell attachment compared to the CTRL, which is typical for electrospun synthetic matrices before full cellular adaptation. It should also be noted that lemon juice, present in cl-PVA-L and cl-PVA-LP, contains citric acid, which can lower the pH of the culture environment. A pH that is too low can destabilize cell membranes and reduce enzymatic activity, negatively impacting cell growth and proliferation. The components of lemon juice can affect various cellular signaling pathways, potentially disrupting normal cellular processes such as the cell cycle and apoptosis. From day 3 onward, more pronounced differences were noted between the samples (Fig. 8a). Comparing the two base groups, the water-spun materials exhibited slightly higher cell viability on day 3 than the highly acidic lemon juice-containing counterparts, confirming that the absence of initial microenvironment acidification favors faster cell recovery. Despite these differences, the cells continued to demonstrate a preference for proliferation, suggesting that all the developed materials are fully biocompatible. Interestingly, it was observed that the incorporation of bromelain into the hydrogels had a greater impact on cell numbers than the presence of water or lemon juice alone. Most importantly, the long-term evaluation on day 7 revealed that the matrices prepared with lemon juice (cl-PVA-L and cl-PVA-LP) exhibited significantly higher cell proliferation and metabolic activity than the corresponding water-spun samples (cl-PVA-W and cl-PVA-WP). This clearly demonstrates that the incorporation of lemon juice components, despite the initial acidification challenge, ultimately provides a more supportive microenvironment for fibroblast growth. Consequently, these findings prove that the lemon juice-modified materials possess an enhanced biocompatibility compared to the standard water-based samples.

Components of lemon juice, such as ascorbic acid, can act as prooxidants under certain conditions, leading to oxidative stress. Excess free radicals can damage DNA, proteins, and lipids in cells, leading to damage or cell death [48]. Citric acid and other compounds can influence protein structure by chelating metal ions, which are cofactors for

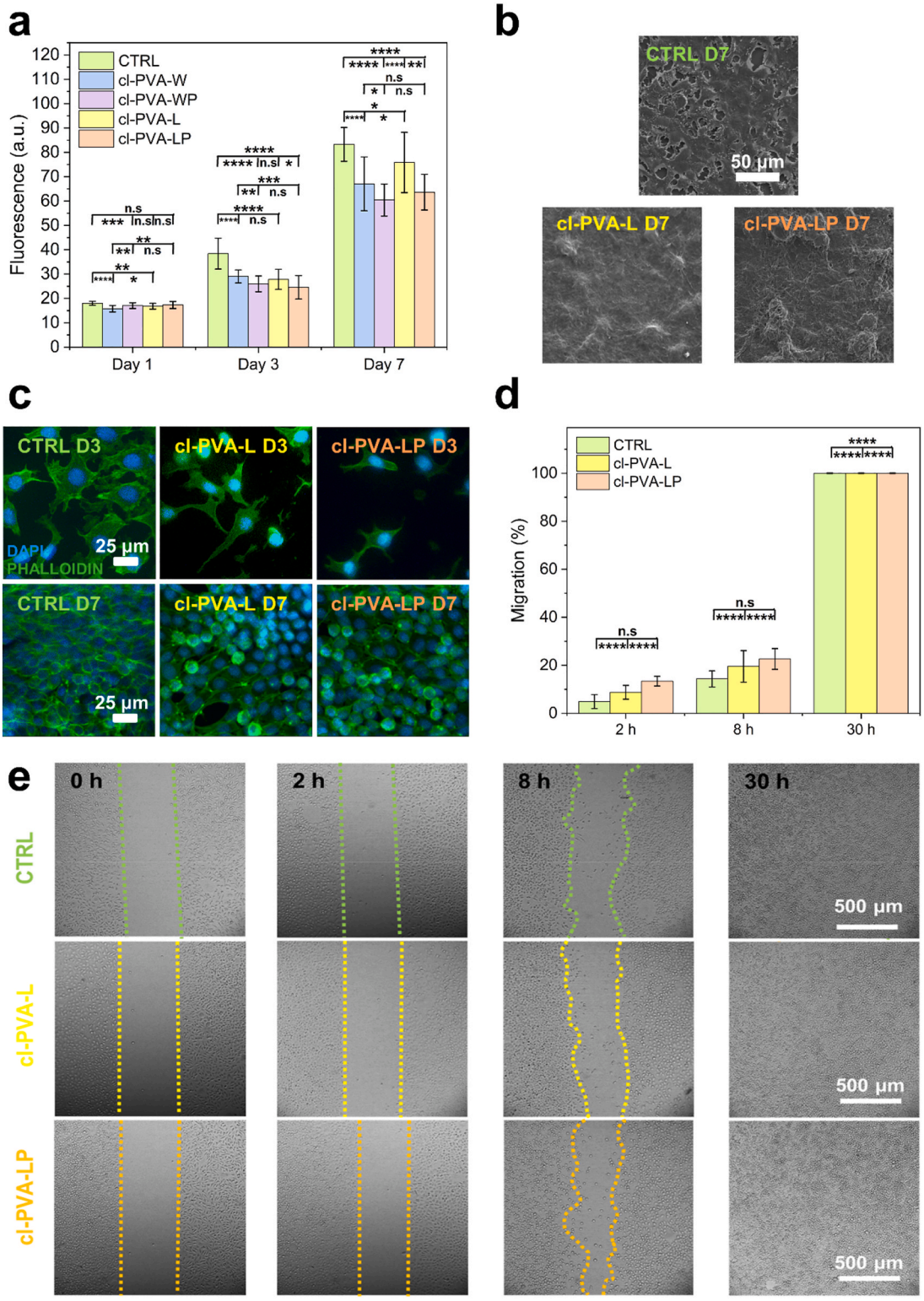

Fig. 8. Biocompatibility and *in vitro* wound healing evaluation of a developed nanofibrous hydrogel. a) Cell proliferation of L929 fibroblast cells seeded on cl-PVA-W, cl-PVA-WP, cl-PVA-L, cl-PVA-LP, and CTRL up to 7 days of culture. b) SEM images of L929 fibroblasts cultured on cl-PVA-L, cl-PVA-LP fibrous samples, and CTRL for 7 days. c) Confocal images of cells seeded on cl-PVA-L, cl-PVA-LP, and CTRL (day 3: cl-PVA-L D3, cl-PVA-LP D3, and CTRL D3; day 7: cl-PVA-L D7, cl-PVA-LP D7, and CTRL D7) and stained with Phalloidin (green color) for cell cytoskeleton visualization and DAPI (blue color) for identifying the cell nuclei. Both materials are fully biocompatible. Over a prolonged culture, the addition of bromelain enhanced cell proliferation compared to lemon-only hydrogels, indicating favorable biological interactions. d) Percentage of cell migration over time and e) representative confocal images of the scratch area during the migration tests for L929 fibroblast treated with cl-PVA-L and cl-PVA-LP extracts, as well as the CTRL group, captured at 0, 2, 8, and 30 h. (For interpretation of the references to color in this figure legend, the reader is referred to the Web version of this article.)

many enzymes [55]. This can disrupt the functioning of key cellular processes. SEM images taken 7 days after seeding clearly demonstrated cell attachment and the formation of a "cell carpet" consisting of densely packed cells. Comparing the cells seeded on fibrous samples (cl-PVA-L and cl-PVA-LP) with those on coverslips, the 3D fibrous structure of the samples revealed cells growing at various heights across the samples, whereas the cells on the flat surface of the coverslips spread out in a single plane (Fig. 8b).

To further explore cell morphology, confocal images of Phalloidin/DAPI-stained samples were analyzed to reveal the cell cytoskeleton and nuclei after 3 and 7 days of culture. Initially, L929 fibroblasts showed a typical spindle shape, with thinner actin forms observed in the cl-PVA-L and cl-PVA-LP samples compared to the CTRL cells. Additionally, at the same incubation time of 3 days, a statistically lower number of cells was observed in these groups (Fig. 8c). After 7 days of incubation, all samples were covered with cells; however, the flat surface on which the L929 fibroblasts were seeded in the CTRL resulted in a more developed cytoskeletal structure. Elongated and interconnected actin fibers of neighboring cells were visible. In the cl-PVA-L and cl-PVA-LP groups, interactions between adjacent cells were also evident, but here, the actin fibers were thinner and more concentrated near the cell nucleus.

To more accurately investigate the migration rate of fibroblast cells, a migration assay was performed using a special chamber with two separate compartments. Once the cells reached full confluence, the dividing barrier was removed, and the time it took for cells from adjacent compartments to merge was examined. A clear acceleration of wound closure was observed in the presence of cl-PVA-LP during the early phase of the scratch assay. After 2 h, cells treated with cl-PVA-LP exhibited visibly enhanced migration into the gap compared with both the CTRL and cl-PVA-L groups. Notably, cl-PVA-L alone also supported cell movement toward the wound area, although its effect was less pronounced than that of cl-PVA-LP. This difference still persisted after 8 h, with cl-PVA-LP maintaining the most advanced migrating front, indicating that the addition of pineapple extract containing bromelain enhances cell migration. By 30 h, the wound area was fully closed in all conditions; however, the early time-point differences highlight the ability of cl-PVA-LP to stimulate and accelerate the initial stages of cell migration (Fig. 8d and e).

4. Conclusions

This work demonstrates the successful development of an eco-friendly, PVA-based nanofibrous hydrogel platform using fresh lemon juice as a natural cross-linker and bromelain, an enzyme derived from pineapple extract, as a biologically active additive with anti-inflammatory properties. The cross-linking approach is fully "green," as it involves an esterification reaction between the –OH groups of the polymer and the –COOH groups of the cross-linking agent, induced by a relatively low and enzyme-safe temperature. This process eliminates the need for toxic chemicals, making the nanoplatform environmentally friendly and consistent with the principles of sustainable biomaterials engineering.

Lemon juice, rich in citric acid, effectively cross-linked electrospun PVA nanofibers during mild heat treatment, creating a stable, water-resistant hydrogel network without compromising the proteolytic activity of bromelain. The cross-linked samples retained their fibrous morphology and became insoluble in PBS, confirming effective material stabilization. The cl-PVA-LP hydrogel exhibited a higher cross-linking density than the cl-PVA-L, and the results clearly demonstrate that the enzyme promotes the cross-linking process.

Furthermore, the developed material exhibited pH-dependent swelling resulting from the presence of carboxyl groups in lemon juice. The bioactive components also demonstrated distinct release profiles: lemon juice was released gradually, whereas bromelain showed a rapid, burst-like release. Importantly, the nanofibrous hydrogel demonstrates a favorable balance between the release of multifunctional substances and the maintenance of structural integrity for at least 21 days under physiological conditions. The simultaneous release of both agents can provide sustained antioxidant and antibacterial effects. Bromelain was shown to enhance activity against *S. Aureus* compared to the material without the enzyme. *In vitro* studies on L929 fibroblasts confirmed the hydrogel's biocompatibility and demonstrated accelerated cell migration in a wound-healing model. Additionally, the nanofibrous hydrogel demonstrated a clear photothermal response to NIR irradiation, suggesting its suitability for controlled, light-directed therapeutic strategies.

The cl-PVA-LP combines bioactive, antioxidant, antibacterial, photothermal, and pH-sensitive properties, making it a promising material for biomedical applications such as wound dressings and controlled drug-release systems. Further studies should include *in vivo* testing, optimization of bromelain release, and evaluation of photothermally assisted wound healing.

CRediT authorship contribution statement

Anna Zakrzewska: Writing – review & editing, Writing – original draft, Methodology, Investigation, Conceptualization. **Zuzanna J. Krysiak:** Writing – review & editing, Methodology, Investigation. **Alicja Kosik-Kozioł:** Writing – review & editing, Methodology, Investigation. **Daniel Rybak:** Writing – review & editing, Methodology, Investigation. **Seyed Shahrooz Zargarian:** Writing – review & editing, Methodology, Investigation. **Michele Zanoni:** Writing – review & editing, Methodology, Investigation. **Chiara Gualandi:** Writing – review & editing, Methodology, Investigation. **Filippo Pierini:** Writing – review & editing, Validation, Supervision, Funding acquisition, Conceptualization.

Declaration of generative AI and AI-assisted technologies in the writing process

During the preparation of this work, the authors used ChatGPT-5.0 (OpenAI) to assist with language refinement. The authors reviewed and edited all content and take full responsibility for the integrity and accuracy of the final manuscript.

Declaration of competing interest

The authors declare that they have no known competing financial interests or personal relationships that could have appeared to influence the work reported in this paper.

Acknowledgements

This work was supported by the National Science Centre (NCN) SONATA BIS Project No. 2020/38/E/ST5/00456. TOC was partially designed using images from Flaticon.com and with Canva; Scheme 1 was created with BioRender; Figs. 1 and 3, and S2 were partially created using images from Flaticon.com. S.S.Z. acknowledges the financial support from Horizon TMA MSCA Postdoctoral Fellowships – European Fellowships (HORIZON-TMA-MSCA-PF-EF) action program under the call MSCA Postdoctoral Fellowships 2021 (HORIZON-MSCA-2021-PF-01), grant agreement No. 101068036, "SuSCoFilter".

Appendix A. Supplementary data

Supplementary data to this article can be found online at https://doi.org/10.1016/j.matchemphys.2026.132830.

Data availability

Data will be made available on request.

References

[1] R. Nagarkar, J. Patel, Polyvinyl alcohol: a comprehensive study, Acta Sci. Pharm. Sci. 3 (4) (2019) 34–44.

[2] G. Paradossi, F. Cavalieri, E. Chiessi, C. Spagnoli, M.K. Cowman, Poly(Vinyl alcohol) as versatile biomaterial for potential biomedical applications, J. Mater. Sci. Mater. Med. 14 (8) (2003) 687–691, https://doi.org/10.1023/a:1024907615244.

[3] L. Rahman, J. Goswami, Poly(Vinyl alcohol) as sustainable and eco-friendly packaging: a review, J. Packag. Technol. Res. 7 (1) (2023) 1–10, https://doi.org/10.1007/s41783-022-00146-3.

[4] Y. Liu, H. Hu, X. Yang, J. Lv, L. Zhou, Z. Luo, Hydrophilic modification on polyvinyl alcohol membrane by hyaluronic acid, Biomed. Mater. 14 (5) (2019) 055009, https://doi.org/10.1088/1748-605X/ab3010.

[5] H. Awada, C. Daneault, Chemical modification of Poly(Vinyl alcohol) in water, Appl. Sci. 5 (4) (2015) 840–850, https://doi.org/10.3390/app5040840.

[6] A. Zakrzewska, P. Nakielski, Y.B. Truong, C. Gualandi, C. Velino, S.S. Zargarian, M. Lanzi, A. Kosik-Kozioł, J. Król, F. Pierini, "green" cross-linking of Poly(Vinyl Alcohol)-Based nanostructured biomaterials: from eco-friendly approaches to practical applications, Wiley Interdiscip. Rev. Nanomed. Nanobiotechnol. 17 (3) (2025) e70017, https://doi.org/10.1002/wnan.70017.

[7] A. Zakrzewska, A. Kosik-Kozioł, S.S. Zargarian, M. Zanoni, C. Gualandi, M. Lanzi, F. Pierini, Lemon juice-infused PVA nanofibers for the development of sustainable antioxidant and antibacterial electrospun hydrogel biomaterials, Biomacromolecules 26 (1) (2025) 654–669, https://doi.org/10.1021/acs.biomac.4c01466.

[8] M. Trinadha Rao, C. Phanindra, M. Yamini, C.H. Prasad, Hydrogels the three dimensional networks: a review, Int. J. Curr. Pharm. Sci. 13 (1) (2021) 12–17, https://doi.org/10.22159/ijcpr.2021v13i1.40823.

[9] J. Maitra, V.K. Shukla, Cross-linking in hydrogels - a review, J. Polym. Sci. 4 (2) (2014) 25–31.

[10] O. Lieleg, K. Ribbeck, Biological hydrogels as selective diffusion barriers, Trends Cell Biol. 21 (9) (2011) 543–551, https://doi.org/10.1016/j.tcb.2011.06.002.

[11] S. Trombino, R. Sole, F. Curcio, R. Cassano, Polymeric based hydrogel membranes for biomedical applications, Membranes 13 (6) (2023) 576, https://doi.org/10.3390/membranes13060576.

[12] M. Ribeiro, M. Simões, C. Vitorino, F. Mascarenhas-Melo, Hydrogels in cutaneous wound healing: insights into characterization, properties, formulation and therapeutic potential, Gels 10 (3) (2024) 188, https://doi.org/10.3390/gels10030188.

[13] S.G. Jin, Production and application of biomaterials based on polyvinyl alcohol (PVA) as wound dressing, Chem. Asian J. 17 (21) (2022) e202200595, https://doi.org/10.1002/asia.202200595.

[14] G.C. Türkoğlu, N. Khomarloo, E. Mohsenzadeh, D.N. Gospodinova, M. Neznakomova, F. Salaün, PVA-based electrospun Materials-A promising route to designing nanofiber mats with desired morphological Shape-A review, Int. J. Mol. Sci. 25 (3) (2024) 1668, https://doi.org/10.3390/ijms25031668.

[15] H.S. Mansur, C.M. Sadahira, A.N. Souza, A.A.P. Mansur, FTIR spectroscopy characterization of poly (Vinyl alcohol) hydrogel with different hydrolysis degree and chemically crosslinked with glutaraldehyde, Mater. Sci. Eng. C 28 (4) (2008) 539–548, https://doi.org/10.1016/j.msec.2007.10.088.

[16] A.S. Elgharbawy, A.-G.M. El Demerdash, W.A. Sadik, M.A. Kasaby, A.H. Lotfy, A. I. Osman, Enhancing the biodegradability, water solubility, and thermal properties of polyvinyl alcohol through natural polymer blending: an approach toward sustainable polymer applications, Polymers 16 (15) (2024) 2141, https://doi.org/10.3390/polym16152141.

[17] A. Zakrzewska, S.S. Zargarian, C. Rinoldi, A. Gradys, D. Jarząbek, M. Zanoni, C. Gualandi, M. Lanzi, F. Pierini, Electrospun Poly(Vinyl Alcohol)-Based conductive semi-interpenetrating polymer network fibrous hydrogel: a toolbox for optimal cross-linking, ACS Mater. Au 3 (5) (2023) 464–482, https://doi.org/10.1021/acsmaterialsau.3c00025.

[18] M.A. Iqbal, S. Gohar, M.S. Miah, R. Minami, J. Xiong, M.N. Sarwar, M. Gopiraman, I.S. Kim, Green, sustainable, and eco-friendly smart halochromic sensor derived from Eggshell membrane-based PVA/Curcumin nanofibers for real-time monitoring of chicken freshness, Mater. Today Sustain. 31 (2025) 101125, https://doi.org/10.1016/j.mtsust.2025.101125.

[19] M. Khalid, M. Farooq, M. Adnan, S. Kobe, G. Mayakrishnan, I.S. Kim, Green and sustainable electrospun Poly(Vinyl Alcohol)/Eggshell nanofiber membrane with lemon-honey for facial mask development, ACS Omega 10 (13) (2025) 12972–12982, https://doi.org/10.1021/acsomega.4c09385.

[20] L.P. Hale, P.K. Greer, C.T. Trinh, C.L. James, Proteinase activity and stability of natural bromelain preparations, Int. Immunopharmacol. 5 (4) (2005) 783–793, https://doi.org/10.1016/j.intimp.2004.12.007.

[21] U. Kansakar, V. Trimarco, M.V. Manzi, E. Cervi, P. Mone, G. Santulli, Exploring the therapeutic potential of bromelain: applications, benefits, and mechanisms, Nutrients 16 (13) (2024) 2060, https://doi.org/10.3390/nu16132060.

[22] R. Pavan, S. Jain, Shraddha, A. Kumar, Properties and therapeutic application of bromelain: a review, Biotechnol. Res. Int. 2012 (2012) 976203, https://doi.org/10.1155/2012/976203.

[23] U. Jančič, S. Gorgieva, Bromelain and nisin: the natural antimicrobials with high potential in biomedicine, Pharmaceutics 14 (1) (2021) 76, https://doi.org/10.3390/pharmaceutics14010076.

[24] N.M. Saptarini, D. Rahayu, I.E. Herawati, Antioxidant activity of crude bromelain of pineapple (Ananas Comosus (L.) Merr) crown from Subang District, Indonesia, J. Pharm. BioAllied Sci. 11 (Suppl 4) (2019) S551–S555, https://doi.org/10.4103/jpbs.JPBS_200_19.

[25] N.C. Praveen, A. Rajesh, M. Madan, V.R. Chaurasia, N.V. Hiremath, A.M. Sharma, In vitro evaluation of antibacterial efficacy of pineapple extract (Bromelain) on periodontal pathogens, J. Int. Oral Health 6 (5) (2014) 96–98.

[26] S.S. Poh, Thermal stability of free bromelain and bromelain-polyphenol complex in pineapple juice, Int. Food Res. J. 18 (3) (2011) 1051–1060.

[27] L.C. de Lencastre Novaes, A.F. Jozala, A.M. Lopes, V. de Carvalho Santos-Ebinuma, P.G. Mazzola, A. Pessoa Junior, Stability, purification, and applications of bromelain: a review, Biotechnol. Prog. 32 (1) (2016) 5–13, https://doi.org/10.1002/btpr.2190.

[28] K. Gao, K. Xu, Advancements and prospects of pH-Responsive hydrogels in biomedicine, Gels 11 (4) (2025) 293, https://doi.org/10.3390/gels11040293.

[29] R. Marrett, D.C.P. Peacock, Strain and stress, J. Struct. Geol. 21 (8–9) (1999) 1057–1063, https://doi.org/10.1016/S0191-8141(99)00020-6.

[30] R.H. Alasfar, S. Ahzi, N. Barth, V. Kochkodan, M. Khraisheh, M. Koç, A review on the modeling of the elastic modulus and yield stress of polymers and polymer nanocomposites: effect of temperature, loading rate and porosity, Polymers 14 (3) (2022) 360, https://doi.org/10.3390/polym14030360.

[31] İ. Gulcin, S.H. Alwasel, DPPH radical scavenging assay, Processes 11 (8) (2023) 2248, https://doi.org/10.3390/pr11082248.

[32] A. Kosik-Kozioł, P. Nakielski, D. Rybak, W. Frączek, C. Rinoldi, M. Lanzi, M. Grodzik, F. Pierini, Adhesive antibacterial moisturizing nanostructured skin patch for sustainable development of atopic dermatitis treatment in humans, ACS Appl. Mater. Interfaces 16 (25) (2024) 32128–32146, https://doi.org/10.1021/acsami.4c06662.

[33] M.A. Norouzi, M. Montazer, T. Harifi, P. Karimi, Flower buds like PVA/ZnO composite nanofibers assembly: antibacterial, in vivo wound healing, cytotoxicity and histological studies, Polym. Test. 93 (2021) 106914, https://doi.org/10.1016/j.polymertesting.2020.106914.

[34] P. Pimpang, S. Rattiphorn, C. Supab, Effect of concentration of citric acid on size and optical properties of Fluorescence Graphene quantum dots prepared by tuning carbonization degree, Chiang Mai J. Sci. 45 (5) (2018) 2005–2014.

[35] M.A. Najim, B.I. Khalil, A.A. Hameed, Characterizing optimum electrospinning conditions for graft urethanized Poly(Vinyl Alcohol)(U-PVA), Heliyon 8 (11) (2022) e11423, https://doi.org/10.1016/j.heliyon.2022.e11423.

[36] S.S. Zargarian, B. Kupikowska-Stobba, A. Kosik-Kozioł, M. Bartolewska, A. Zakrzewska, D. Rybak, K. Bochenek, M. Osial, F. Pierini, Light-responsive biowaste-derived and bio-inspired textiles: dancing between bio-friendliness and antibacterial functionality, Mater. Today Chem. 41 (2024) 102281, https://doi.org/10.1016/j.mtchem.2024.102281.

[37] Y. Yu, P. Lin, Y. Zhao, C. Liu, C. Xu, X. Sun, L. Liang, J. Wang, P. Liu, Preparation and performance characterization of novel PVA blended with fluorinated polyimide membrane for gas separation, High Perform. Polym. 33 (4) (2021) 394–404, https://doi.org/10.1177/0954008320959708.

[38] S.S. Zargarian, S. Suárez-García, J. Saiz-Poseu, L. Zuppiroli, M. Lanzi, D. Ruiz-Molina, F. Pierini, Light-activated superhydrophobicity of sustainable micro-structured spent coffee grounds-based interfaces via fatty acids modulation, ChemSusChem 18 (10) (2025) e202402254, https://doi.org/10.1002/cssc.202402254.

[39] F. Cadet, C. Robert, B. Offmann, Simultaneous determination of sugars by multivariate analysis applied to mid-infrared spectra of biological samples, Appl. Spectrosc. 51 (3) (1997) 369–375, https://doi.org/10.1366/0003702971940224.

[40] J.P. Lommerse, L.M. Kroon-Batenburg, J.P. Kamerling, J.F. Vliegenthart, Conformational analysis of the Xylose-containing N-Glycan of pineapple stem bromelain as part of the intact glycoprotein, Biochemistry 34 (25) (1995) 8196–8206, https://doi.org/10.1021/bi00025a027.

[41] R. Esfandiary, J.S. Hunjan, G.H. Lushington, S.B. Joshi, C.R. Middaugh, Temperature dependent 2nd derivative absorbance spectroscopy of aromatic amino acids as a probe of protein dynamics, Protein Sci. 18 (12) (2009) 2603–2614, https://doi.org/10.1002/pro.264.

[42] N.C. Li, P. Tang, R. Mathur, Deuterium isotope effects on dissociation constants and formation Constants[1], J. Phys. Chem. 65 (6) (1961) 1074–1076, https://doi.org/10.1021/j100824a521.

[43] R. Shi, J. Bi, Z. Zhang, A. Zhu, D. Chen, X. Zhou, L. Zhang, W. Tian, The effect of citric acid on the structural properties and cytotoxicity of the polyvinyl Alcohol/Starch films when molding at high temperature, Carbohydr. Polym. 74 (4) (2008) 763–770, https://doi.org/10.1016/j.carbpol.2008.04.045.

[44] A.S. Singha, H. Kapoor, Effects of Plasticizer/Cross-linker on the mechanical and thermal properties of Starch/PVA blends, Iran. Polym. J. 23 (8) (2014) 655–662, https://doi.org/10.1007/s13726-014-0260-9.

[45] B.J. Holland, J.N. Hay, The thermal degradation of Poly(Vinyl alcohol), Polymer 42 (16) (2001) 6775–6783, https://doi.org/10.1016/S0032-3861(01)00166-5.

[46] S.L. Jacques, Optical properties of biological tissues: a review, Phys. Med. Biol. 58 (11) (2013) R37–R61, https://doi.org/10.1088/0031-9155/58/11/R37.

[47] M.E. Darvin, Optical methods for non-invasive determination of skin penetration: current trends, advances, possibilities, prospects, and translation into in vivo human studies, Pharmaceutics 15 (9) (2023) 2272, https://doi.org/10.3390/pharmaceutics15092272.

[48] S. Ali, Lemon juice antioxidant activity against oxidative stress, Baghdad Sci. J. 17 (2020) 207, https://doi.org/10.21123/bsj.2020.17.1(Suppl.).0207, 1(Suppl.).

[49] F.M. El-Demerdash, D.M. Hussien, N.F. Ghanem, A.M. Al-Farga, Bromelain modulates liver injury, hematological, molecular, and biochemical perturbations induced by aluminum via oxidative stress inhibition, Biomed Res. Int. 2022 (2022) 5342559, https://doi.org/10.1155/2022/5342559.

[50] N. Akaras, E. Toktay, H. Şimşek, N. Aydemir Celep, N. Yüce, Deneysel sıçan sepsis modelinde bromelainin oksidatif stres ve Akciğer Doku Histopatolojisi Üzerine

etkileri, Kocatepe Vet. J. 16 (3) (2023) 252–259, https://doi.org/10.30607/kvj.1302701.
[51] S. Agarwal, B. Chaudhary, R. Bist, Bacoside A and bromelain relieve dichlorvos induced changes in oxidative responses in mice Serum, Chem. Biol. Interact. 254 (2016) 173–178, https://doi.org/10.1016/j.cbi.2016.05.017.
[52] S.B. Kedare, R.P. Singh, Genesis and development of DPPH method of antioxidant assay, J. Food Sci. Technol. 48 (4) (2011) 412–422, https://doi.org/10.1007/s13197-011-0251-1.
[53] E.I. Oikeh, E.S. Omoregie, F.E. Oviasogie, K. Oriakhi, Phytochemical, antimicrobial, and antioxidant activities of different citrus juice concentrates, Food Sci. Nutr. 4 (1) (2016) 103–109, https://doi.org/10.1002/fsn3.268.
[54] Z. Zhang, M. Cao, Z. Shang, J. Xu, X. Chen, Z. Zhu, W. Wang, X. Wei, X. Zhou, Y. Bai, J. Zhang, Research progress on the antibacterial activity of natural flavonoids, Antibiotics (Basel) 14 (4) (2025) 334, https://doi.org/10.3390/antibiotics14040334.
[55] D. Fernández, E. Boix, I. Pallarès, F.X. Avilés, J. Vendrell, Structural and functional analysis of the complex between citrate and the zinc peptidase carboxypeptidase A, Enzym. Res. 2011 (2011) 128676, https://doi.org/10.4061/2011/128676.